QC
807.5
.U6
A5
no.85
c.2

NOAA Technical Memorandum ERL AOML-85

MEASUREMENT OF FUGACITY OF CARBON DIOXIDE IN SEAWATER: AN EVALUATION OF A METHOD BASED ON INFRARED ANALYSIS

H. Chen
R. Wanninkhof
R.A. Feely
D. Greeley

Atlantic Oceanographic and Meteorological Laboratory
Miami, Florida
August 1995

noaa NATIONAL OCEANIC AND ATMOSPHERIC ADMINISTRATION / Environmental Research Laboratories

QC
8075
.U6
A5
no.85
c.2

NOAA Technical Memorandum ERL AOML-85

MEASUREMENT OF FUGACITY OF CARBON DIOXIDE IN SEAWATER: AN EVALUATION OF A METHOD BASED ON INFRARED ANALYSIS

Hua Chen
Rik Wanninkhof

Atlantic Oceanographic and Meteorological Laboratory

Richard A. Feely
Dana Greeley

Pacific Marine Environmental Laboratory
Seattle, Washington

Atlantic Oceanographic and Meteorological Laboratory
Miami, Florida
August 1995

LIBRARY
JAN 30 1996
N.O.A.A.
U.S. DEPT. OF COMMERCE

UNITED STATES
DEPARTMENT OF COMMERCE

Ronald H. Brown
Secretary

NATIONAL OCEANIC AND
ATMOSPHERIC ADMINISTRATION

D. JAMES BAKER
Under Secretary for Oceans
and Atmosphere/Administrator

Environmental Research
Laboratories

James L. Rasmussen
Director

NOTICE

Mention of a commercial company or product does not constitute an endorsement by the NOAA Environmental Research Laboratories. Use of information from this publication concerning proprietary products or the tests of such products for publicity or advertising purposes is not authorized.

For sale by the National Technical Information Service, 5285 Port Royal Road, Springfield, VA 22061

Table of contents

Abstract

An analysis system is described to measure the fugacity of CO_2 (fCO_2)[1] in 500 mL of seawater (discrete samples) by infrared analysis. The unit is used on oceanographic research cruises sponsored by the Ocean-Atmosphere Carbon Exchange Study (OACES) of NOAA since 1991 for a total of approximately 10,000 measurements. The precision of the analyses based on replicate samples during routine analysis is 0.2 %. Precision is primarily limited by sample storage, and the difference between headspace gas and water CO_2 concentrations prior to equilibration. The precision and accuracy of the instrument is estimated in several different ways. A preliminary side by side test of two different discrete fCO_2 systems using an infrared (IR) analyzer and a gas chromatograph (GC) show a variability of 0.8 % without significant bias. For surface waters the discrete measurements are compared with measurements from a continuous flowing underway system which was deployed on all cruises. Select comparisons with fCO_2 calculated from spectrophotometric pH and DIC (Total Dissolved Inorganic Carbon) measurements are performed. These comparisons are limited by the uncertainty in the magnitude and the temperature dependence of the carbon and borate dissociation constants. Indirect comparisons are made with pCO_2 measurements of Drs. Takahashi and Chipman of LDEO in the South Atlantic and Equatorial Pacific (EqPac). Although the measurements were performed months (for the EqPac study in 1992) to years (for the South Atlantic study in 1989 and 1991) apart, some inferences can be made by normalizing the fCO_2 values and by performing the comparison in property space. The comparison indicates that the precision of our system is comparable to that of the LDEO system. The surface values obtained from the LDEO system during EqPac are 1.5 to 3% lower. There is inconclusive evidence that some of the subsurface LDEO pCO_2 values are lower as well. However, the comparison of subsurface values for the North Atlantic Deep Water in the South Atlantic study shows good agreement. Because of the current uncertainty in dissociation constants there is no *a priori* way to determine which value is correct.

---

[1]The fugacity of CO_2 is the partial pressure corrected for non-ideality of interaction between CO_2 and N_2/O_2. Fugacity is 0.7 to 1.2 µatm lower than the corresponding partial pressure and depends primarily on temperature.

Introduction

The role of the ocean in modulating atmospheric anthropogenic CO_2 increases is poorly constrained [*Conway et al.*, 1994; *Sarmiento*, 1991; *Tans et al.*, 1990]. The vast size of the ocean, lack of accuracy in the measurement of oceanic carbon system parameters, and seasonal variability in the upper several hundred meters of the ocean are the main reasons that the oceanic sink for CO_2 is uncertain. Several large research programs were initiated in the last decade to address these problems. The Joint Global Ocean Flux Study (JGOFS) endorsed aquatic carbon dioxide measurements on the one-time hydrographic sections of the World Hydrographic Programme (WHP) of the World Ocean Circulation Experiment (WOCE). The inorganic carbon measurements on these cruises which are sponsored by the department of energy (DOE) will yield a "snapshot" of the oceanic total carbon inventory. A major objective of the ocean-atmosphere carbon exchange study (OACES) of the climate and global change program (C&GC) of NOAA is to perform inorganic carbon system parameter measurements on repeat transects in each major ocean basin on five to ten year intervals. The measurements will indicate how the oceanic carbon system is changing in response to the atmospheric anthropogenic burden and how much anthropogenic carbon is sequestered by the ocean.

To accomplish these goals, long term accuracy and a better understanding of the oceanic inorganic carbon system is imperative. Intercalibration exercises, uniform instruments, and, in particular, use of traceable liquid reference materials have greatly improved the accuracy of total dissolved inorganic carbon (DIC) measurements [*DOE*, 1994]. To separate natural changes in the oceanic carbon system from man-induced changes other carbon system parameters aside from DIC must be determined. These parameters can include stable carbon isotopes of DIC [*Quay et al.*, 1992], pH [*Byrne and Breland*, 1989], Total Alkalinity [*Dickson*, 1981; *Millero et al.*, 1993], and fugacity of CO_2 (fCO_2) [*Chipman et al.*, 1993; *Wanninkhof and Thoning*, 1993]. In particular, changes in DIC arising from the oceanic biological cycle must be separated from changes caused by the air-sea flux of CO_2. Changes in the biological cycle will leave a distinctly different carbon signature in the ocean than atmospheric CO_2 input. This can be illustrated in a simplistic manner by the perturbation of fCO_2 and DIC by biological respiration versus anthropogenic input [2]. On first order DIC increases by respiration will be accompanied by fCO_2 increases in the ratio DIC : fCO_2 = 1: 1.3 . DIC increases caused by invasion of atmospheric CO_2 will manifest itself by a ratio of DIC : fCO_2 = 1: 2.1. Thus by measuring the change in fCO_2 and DIC over time anthropogenic input can be determined and separated from variability in the biological system. Of course, the quantitative separation between a-biotic and biotic CO_2 increase must utilize other chemical and physical parameters such as density, nitrate, TAlk, pH, and carbon isotopes. Each carbon system parameter has its intrinsic advantages and disadvantages, in dynamic range, ease of measurement, and ease of interpretation. For a robust estimate of carbon uptake by the ocean several of the parameters must be measured together.

Measurement of fugacity as a carbon system parameter has several advantages and some experimental pitfalls. At constant temperature the dynamic range of fCO_2 in ocean water

---

[2]In this example we assume that sea surface temperature is 20 ^{o}C, the salinity is 35, and DIC changes from 1950 to 1975 μmol kg^{-1}. For the anthropogenic input, total alkalinity (TAlk) is assumed to remain constant while for the case of respiration, the alkalinity increases by 10 μEq kg^{-1}, corresponding to a hard tissue to soft tissue ratio of 1: 4. The contribution of nitrate to TAlk is ignored.

is three to four times that of DIC. Precision of the analyses described, expressed in terms of dynamic range, is currently about two times less than for DIC (1 % vs. 0.5 %). The main difficulty with fCO_2 measurements is that the measurement is done in the gas phase. The gas in the water must be equilibrated with gas in a headspace prior to analysis. This equilibration perturbs the fCO_2 in the water, and must be accounted for. In this respect spectrophotometric pH are preferable as a carbon system parameter. However, in order to convert pH to a parameter of direct relevance to the inorganic carbon system such as fCO_2, one must have an accurate knowledge of the carbon dissociation constants, the influence of minor acids on seawater pH, the temperature dependence of pH, and the pH of the indicator solutions. For fCO_2 measurements only the temperature dependence of fCO_2 plays a major role in interpretation. The precision of pH and fCO_2 measurements are better than TAlk, which translates into a better constraint on the inorganic aquatic carbon system.

System description

The discrete fCO_2 system (Figure 1) is patterned after the setup described in *Chipman et al.* [1993] and is discussed in detail in *Wanninkhof and Thoning* [1993]. The major difference between the systems is that our system uses a LI-COR™ (model 6262) non-dispersive infrared analyzer, while the system of *Chipman et al.* [1993] utilizes a gas chromatograph with a flame ionization detector and a methanizer which quantitatively converts CO_2 into CH_4 for analysis.

Samples collected in 500-mL volumetric flasks are brought to a temperature of 20.00±0.02 °C, by first inserting the flasks in a pre-bath at 19-21 °C and subsequently in a Nestlab™ (model RT-220) controlled temperature bath for equilibration and analysis. A 60-mL headspace is created in the sample flask by displacing the water using a compressed standard gas with a CO_2 mixing ratio close to the fCO_2 of the water. The headspace is circulated in a closed loop through the infrared analyzer which measures CO_2 and water vapor levels in the sample cell. The headspaces of two flasks are equilibrated simultaneously in channels A and B. While headspace from the flask in channel A goes through the IR analyzer, the headspace of the flask in channel B is recirculated in a closed loop. The samples are equilibrated till the running mean of twenty consecutive 1-second reading from the analyzer differ by less than 0.1 ppm., which on average takes about 10 minutes. An expandable volume consisting of a balloon keeps the content of flasks at room pressure.

In order to maintain measurement precision, a set of six gas standards is run through the system after every eight to twelve seawater samples. The standards have mixing ratios of 201.4, 354.1, 517.0, 804.5, 1012.2, and 1529 ppm (or 2020 ppm for work in the Equatorial Pacific) which bracket the fCO_2 at 20 °C ($fCO_2(20)$) values observed in the water column.

The determination of $fCO_2(20)$ in water from the headspace measurement involves several steps. The IR detector response for the standards is normalized for temperature, the IR analyzer voltage output for samples are normalized to 1 atm. pressure, and the IR detector response is corrected for the influence of water vapor. The sample values are converted to a mixing ratio based on the compressed gas standards. The mixing ratio in the headspace is converted to fugacity and corrected to fugacity of CO_2 in the water sample prior to equilibration by accounting for change in total CO_2 in water during the equilibration process (for details see, Wanninkhof and Thoning, [1993]). The change in $fCO_2(20)$ caused by the change in DIC is calculated using the constraint that TAlk

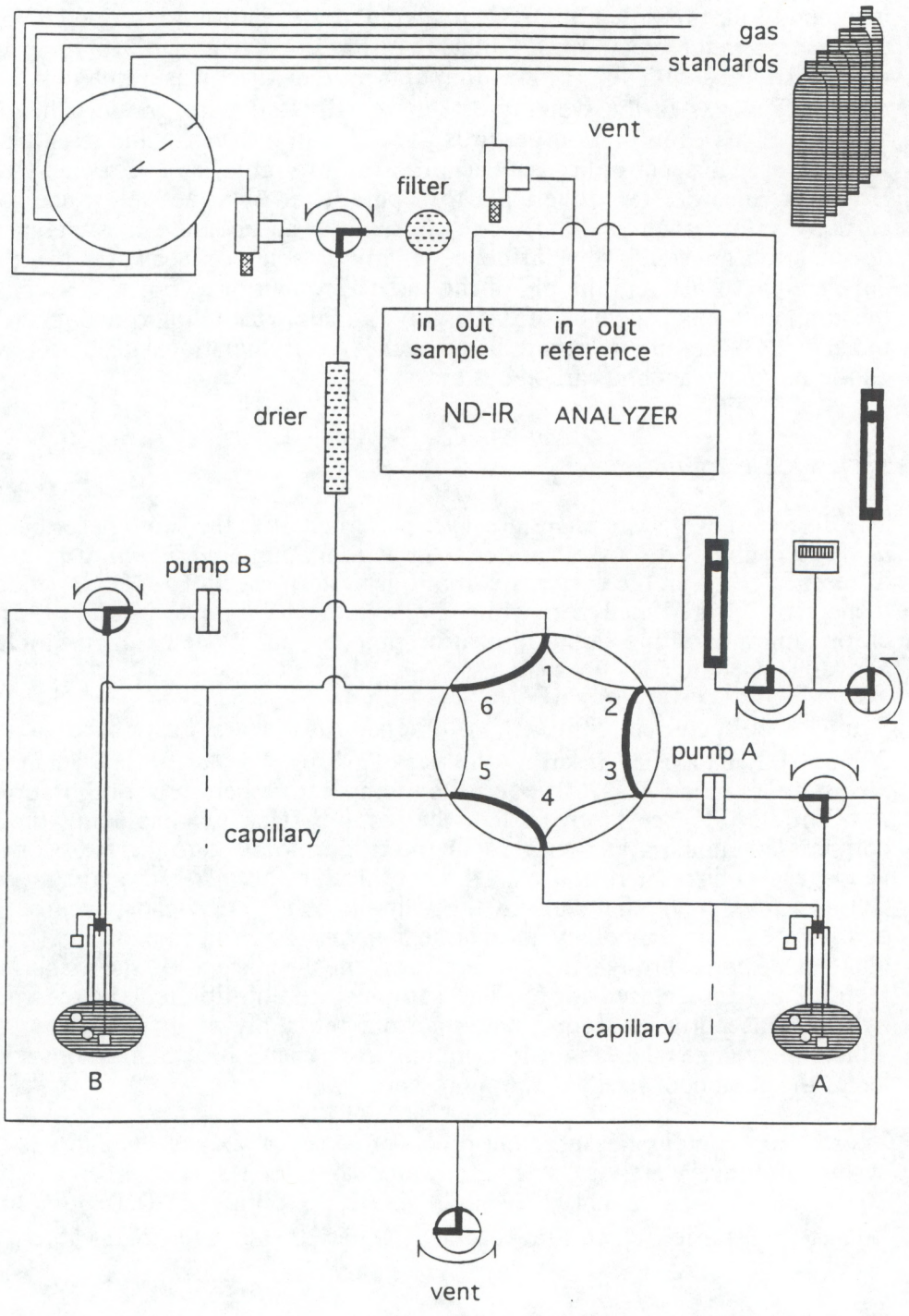

Figure 1. Schematic of the discrete fCO_2 system. The normally open position of the solenoid valves is shown as a bold line in the valve. The arrows above the valve indicate which ports are connected in the open position. For a full description see *Wanninkhof and Thoning* [1993].

remains constant during exchange of CO_2 gas between the headspace and the water. The calculation is outlined in the appendix of *Peng et al.*, [1987].

System performance

The precision of the analysis is influenced by IR detector response, variations in pressure and IR detector temperature, the water vapor correction, and the correction for CO_2 exchange between water and headspace during equilibration.

Response to gas standards

The infrared analyzer shows a non-linear response to increasing CO_2 concentrations which degrades the performance at high concentrations. Figure 2 shows a typical response curve for the IR detector and the change in sensitivity of the detector (expressed as the change in mV IR detector output per ppm CO_2). Over the experimental range the sensitivity decreases by a factor of four. To mitigate the loss of response at high CO_2 levels, the detector is run in differential mode with the 350 ppm standard acting as the reference gas. Typical instrument noise level based on 30 consecutive readings of the gas in the detector during sample analysis is 0.2 mV. This translates to 0.05 ppm at 350 ppm and to 0.2 ppm for a sample of 2000 ppm.

Variation in pressure and temperature

Detector response is influenced by temperature and pressure fluctuations in the IR detector. These variations are corrected for by using an algorithm provided by the instruction manual [*LI-COR*, 1990]. The voltage (V) response is related to pressure by: $V_{p1} = V_{p2}\,(P_1/P_2)$. The temperature response is related to the mixing ratio (X) by: $X_{T1} = X_{T2}\,(T_2/T_1)$, where T is in K. The samples are bracketed by a series of standards, and pressure and temperature fluctuations are generally small between standards. For example, for leg 1 of the N. Atlantic cruise in 1993 (N.ATL-93) the average deviation of IR detector temperature between standards bracketing a series of standards was 0.5 °C for 60 runs, and the average pressure deviation was 0.9 mB. The variation in average voltage response for the six standards is given in Table 1. As indicated below these variations in instrument response have a minor influence on the overall uncertainty.

Water vapor correction

Since gas standards are dry and samples are saturated with water at 20 °C, a water vapor correction must be applied. The correction for water vapor in the IR analyzer is done empirically. Water vapor influences the CO_2 signal of the IR analyzer in three different ways: direct absorption in the CO_2 wave band (this IR detector is focused at 4.26 micron using a 150 nm bypass filter), pressure broadening, and dilution. Since pressure broadening is difficult to determine on a theoretical basis, all three effects are corrected for simultaneously by determining an empirical fit between IR analyzer response of the six standards with different levels of water vapor using the readings from the H_2O channel and the CO_2 channel.

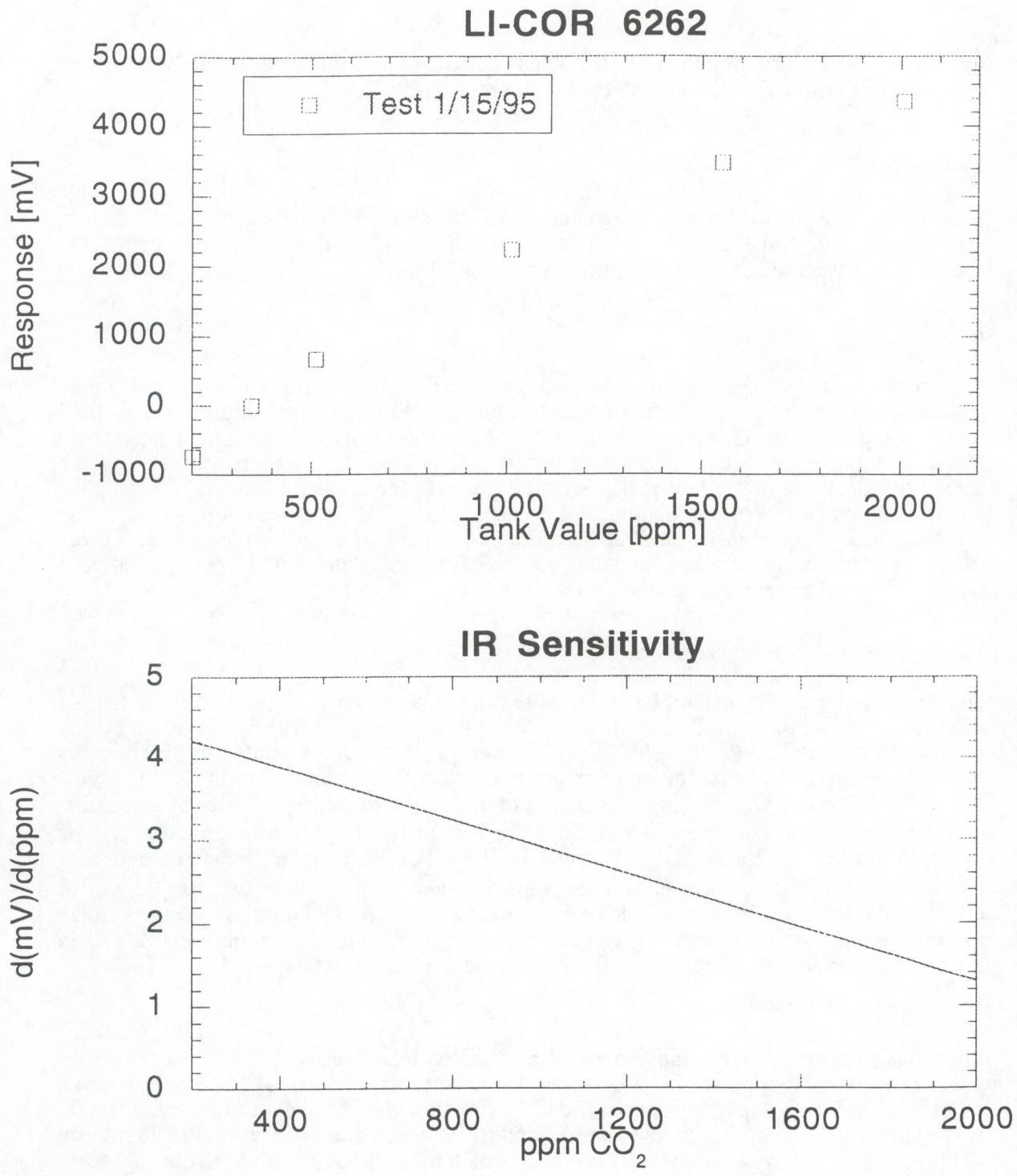

Figure 2. Top: typical response curve of the IR detector to different gas standards. Bottom: change in response with increasing concentrations. Note the fourfold decrease in sensitivity over the operational range of the IR detector.

Table 1. Response of IR analyzer to different gas standards, and variation of temperature and pressure of cell during subsequent analyses for leg 1 of the N.ATL-93 cruise[1].

STD #	CO_2 [ppm]	Av. resp. [mV]	±	Pres. [mB]	±	IR temp [°C]	±
2	187.69	-1009.60	2.45	1014.06	0.93	33.65	0.49
1	352.54	9.81	1.45	1014.06	0.86	33.65	0.49
6	511.93	803.67	1.25	1014.03	0.92	33.65	0.48
3	804.52	2004.06	2.66	1014.04	0.92	33.6	0.49
5	1189.35	3249.26	4.04	1014.02	0.93	33.65	0.48
4	1552.78	4230.13	4.92	1014.03	0.91	33.65	0.49

STD #: sequence in which standards are run
CO_2 [ppm]: mixing ratio of CO_2 in standard tank
Av. resp. [mV]: average response of IR detector based on 60 comparisons over three weeks
±: average absolute difference of response for standards bracketing a set of 12 samples (in mV)
Pres.: average atmospheric pressure based on 60 comparisons over three weeks
±: average absolute difference of atmospheric pressure for standards bracketing a set of 12 samples (in mV)
IR temp: average temperature of IR analyzer based on 60 comparisons over three weeks
±: average absolute difference of IR analyzer temp for standard runs bracketing a set over 12 samples (in mV)

[1]The absolute difference shows the drift between two sets of standards. In reducing the data, a linear extrapolation is performed between standards bracketing the sample to determine the appropriate mixing ratio for the headspace. The average absolute difference gives an indication of the change in standard response during the time 12 samples are run time (approximately 2 hours).

The correction is of the form:

$$mV'CO_{2,dry} = mV'CO_2 + g(mV'CO_2)\ mVH2O$$

and

$$g(mV'CO_2) = 2.2913 \times 10^{-2} + 4.6634 \times 10^{-6}\ mV'CO_2 - 3.876 \times 10^{-10}\ (mV'CO_2)^2$$

where $mV'CO_{2,dry}$ is the millivolt output of the IR analyzer for dry air normalized to 1013.25 mB. This algorithm is checked yearly and has not changed significantly over time. The typical response of the water vapor channel to water saturated air is 2000 mV. Thus the correction from wet to dry will be about 40 mV (≈ 10 ppm) for a 350 ppm and 70 mV (≈ 50 ppm) for a 2000 ppm headspace.

Comparison of our normalization scheme with the LI-COR 6262 correction algorithm

Although only "raw" IR detector response is used for the determination of fCO_2 values, it is of interest to compare the results with the algorithms built into the detector. The LI-COR 6262 has a built-in correction algorithm for the conversion from mV output to mixing ratio, and an algorithm to correct for the influence of water vapor (both dilution and pressure band broadening). Both algorithms are empirically determined by the manufacturer. The standard response is fit to a fifth-order polynomial and yearly factory redetermination of the constants is recommended. Both the water vapor correction and standard response algorithms require zeroing of the detector by flowing gases with the same CO_2 and H_2O concentration through the reference and sample cell, and setting of the "span" using gases with known CO_2 and H_2O concentration. Figure 3 shows the difference in mixing ratio determined from the LI-COR 6262 and the calibrated compressed gas tank values. The zero gas used in the calibration was 348.38 ppm, and the span gas was 2020 ppm. All the differences are within ± 0.3% of the fCO_2 values of gas tanks. There is good agreement between our fit and the algorithms provided by LI-COR despite the fact that the IR detector had not been recalibrated by the manufacturer for two years. The compressed gas standards used in the comparison were CO_2 in O_2/N_2 mixtures (synthetic air) obtained commercially. They were calibrated against four compressed gas standards from the laboratory of Dr. Keeling of SIO with mixing ratios of: 203.92, 350.44, 794.94, and 1502.86 ppm in natural air.

The LI-COR 6262 water vapor algorithm appears acceptable as well. The water vapor channel exhibits significant short term drift making zeroing and "spanning" the water vapor channel problematic. The span was set using a LI-COR model 602 water vapor generator. Figure 4 shows the response of the IR detector for the dry standard and for a standard saturated with water by flowing the gas through a small aliquot of acidified water at 20 °C. The difference between the dry gas and "wet" gas corrected to dry conditions is -0.5 to -2.5 ppm. The negative trend is attributed to a drift in the span. The uncorrected difference between wet and dry CO_2 output signal ranges from -35 to -65 mV (or about 10 to 50 ppm). Thus the internal calibration for water vapor is effective in correcting for most of the water vapor effect.

Exchange of CO_2 with headspace during equilibration

The equilibration of fCO_2 of the water sample with the headspace perturbs the $fCO_2(20)$ of the water if it differs from the fCO_2 in the headspace. The perturbation is a function of the headspace to water volume ratio, and the fugacity difference between headspace and water. The $fCO_2(20)$ values in water prior to equilibration can be calculated from the water sample and headspace volume, the fCO_2 in the headspace before and after equilibration, and the DIC of the water . From the fCO_2 in the headspace and DIC after equilibration the TAlk is calculated. Since the TAlk does not change during equilibration, the TAlk and DIC before equilibration are used to calculate the $fCO_2(20)$ in the water sample before equilibration.

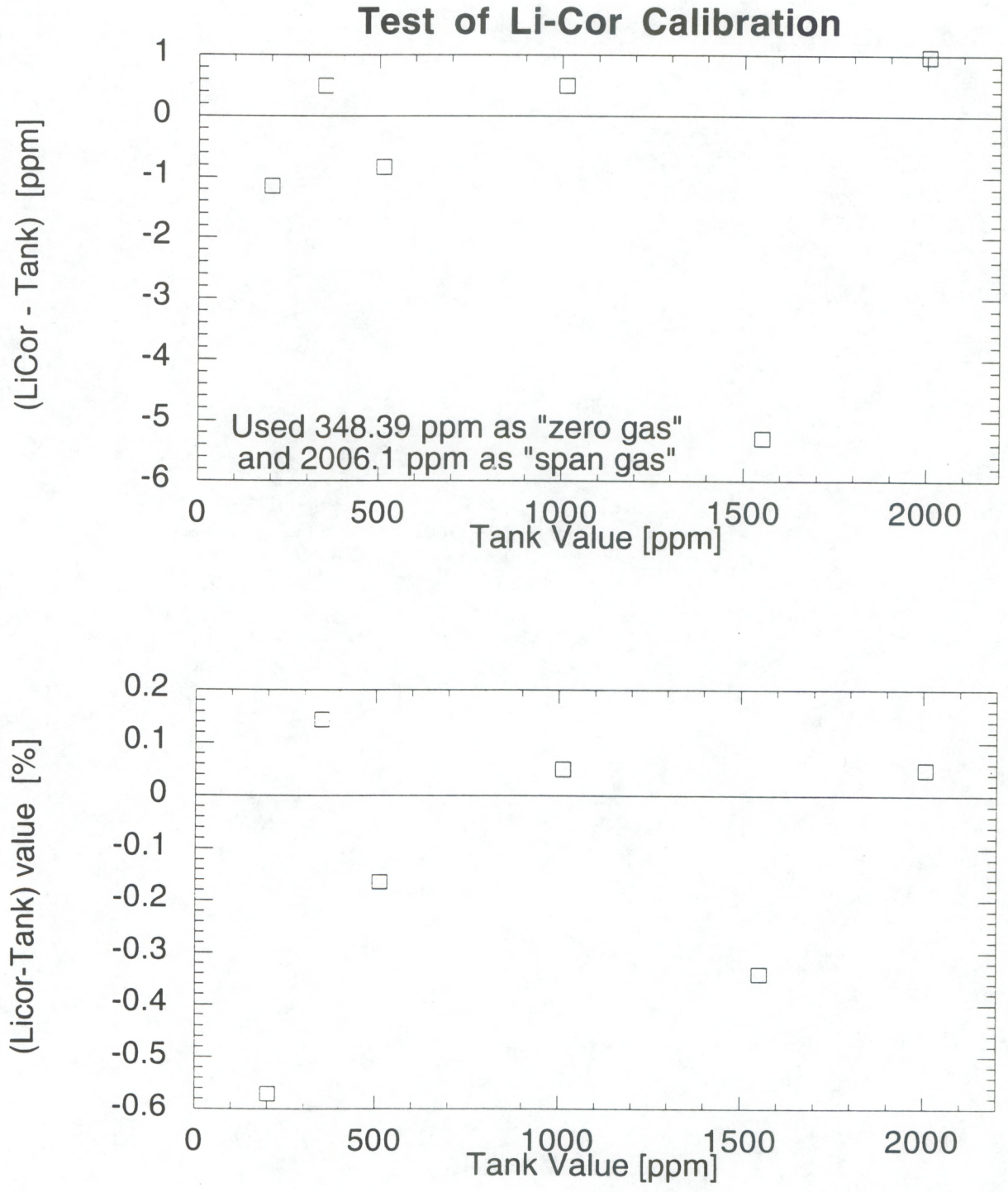

Figure 3. Top: comparison of the internal calibration of the IR detector and the absolute tank calibration, expressed as the difference between the LI-COR IR detector value and the tank value (calibrated against WMO referenced gases). This example illustrates that the empirical algorithm supplied with the detector is quite accurate.
Bottom: same as top figure except expressed as percent of the corresponding standard value

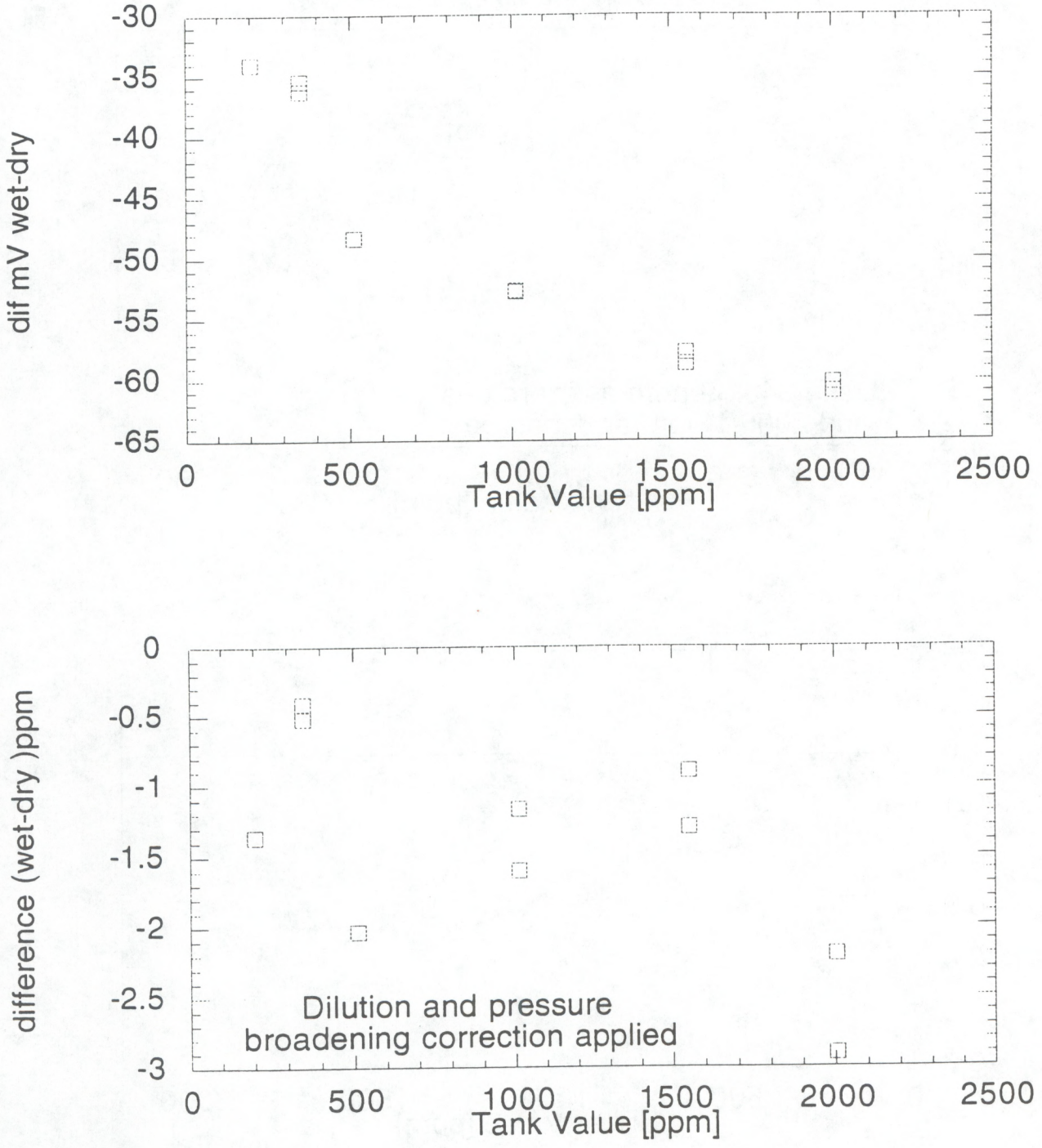

Figure 4. Top: Difference in response of the IR detector to dry and water saturated (20 ^{o}C) standard gases.
Bottom: Difference in response (in ppm) after the instrumental water vapor correction is applied to the moist gas, illustrating that the correction is quite robust. Note that in our work we do not rely on either the instrumental water vapor correction or internal conversion from detector response (in mV) to mixing ratio.

Figure 5 shows the maximum errors introduced by uncertainties in the headspace volume when the headspace gases were chosen which were far from equilibrium. Two examples are presented; N. Atlantic surface water and Pacific 1000-m water. Estimated uncertainty in the water volume measurements is 1 mL and contributes 2 ppm uncertainty for the intermediate water but less than 0.1 ppm for surface water. The difference is caused by the smaller buffering factor for the intermediate water such that a same amount change in DIC will correspond to a greater $fCO_2(20)$ change.

The change in fCO_2 in water due to equilibration can be minimized by choosing a headspace gas close to the estimated $fCO_2(20)$ of the water. For this reason six compressed gas standards with differing CO_2 mixing ratios are available to create the headspace. Figure 6 gives the correction to the fCO_2 of the headspace to obtain the corresponding $fCO_2(20)$ in the water as a function of headspace gas. The correction for Pacific 1000-m water, which has a fCO_2 of 1550 µatm, is 180 µatm if a 200 ppm headspace gas is used. For the N.Atlantic surface water with $fCO_2(20)$ of 250 µatm the change is much smaller because of its greater buffering capacity. Since the uncertainty in the correction will be proportional to its magnitude, it can be significant if the headspace is far removed from $fCO_2(20)$ of the water, especially for deep water.

Comparison with other investigations

The performance of the discrete fCO_2 system is compared with four other methods of fCO_2 determination:

a. Results from a newly developed discrete fCO_2 system using a gas chromatograph were compared with the IR analyzer based system on a short cruise across the Florida Straights in 1995.

b. On all the cruises surface water fCO_2 values were measured at one-hour intervals from water obtained through a bow pump at 6-meter depth. These values are compared to the samples taken from the top Niskin bottle (0 to 6-m). The underway fCO_2 values are measured near (± 0.2 °C) sea surface temperature (SST) and corrected to SST. For this comparison the fCO_2 discrete values which are analyzed at 20.00 °C have to be corrected to SST. This correction is a function of which carbon dissociation constants are used.

c. $fCO_2(20)$ values from the 1991 S. Atlantic cruise, and the 140 °W transect of the (boreal) spring and (boreal) fall 1992 EqPac cruises are compared with measurements made close in time by the LDEO group of Drs. Archer, Chipman and Takahashi who have performed fCO_2 analysis using a GC for the last decade.

d. For the 140 °W transect of the spring and fall 1992 EqPac cruises pH values obtained by Dr. Byrne of the University of South Florida (USF) are converted to $fCO_2(20)$ values using DIC.

The dissociation constants to the calculate or correct fCO_2 for the different comparisons are shown in Table 2. There still remains much controversy regarding which constants do the best job converting between the different carbon species [*Dickson and Millero*, 1987; *Millero et al.*, 1993; *Takahashi et al.*, 1993; *Lee, et al.* in preparation, 1995]. As an illustration of the influence of different constants on determining $fCO_2(20)$ from pH and DIC, and correcting $fCO_2(20)$ to fCO_2 *in situ*, calculations using three combinations of

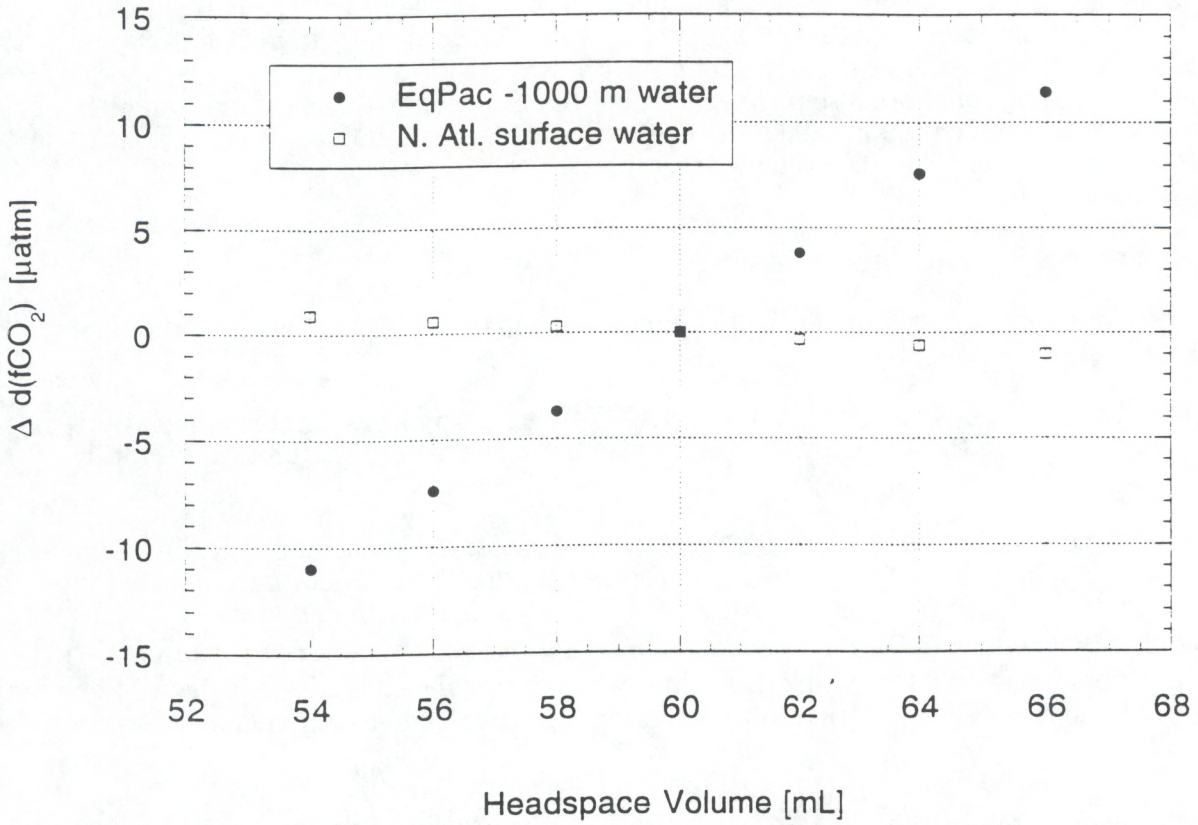

Figure 5. Change of fCO_2 in the equilibrated headspace caused by error of measurement of headspace volume. For this example, the EqPac 1000-m water has a $fCO_2(20)$ of 1550 µatm and a displacement gas of 200 ppm. For the N.ATL. surface water the $fCO_2(20)$ is about 250 µatm and a displacement gas of 1500 ppm is used. The difference sensitivity to headspace volume is because the intermediate water is poorly buffered. In this example it is assumed that 60 mL is the correct headspace volume. The error in measuring the headspace volume is estimated to be 1 mL, contributing at most 2 µatm uncertainty in the final result if the worst displacement gas is chosen.

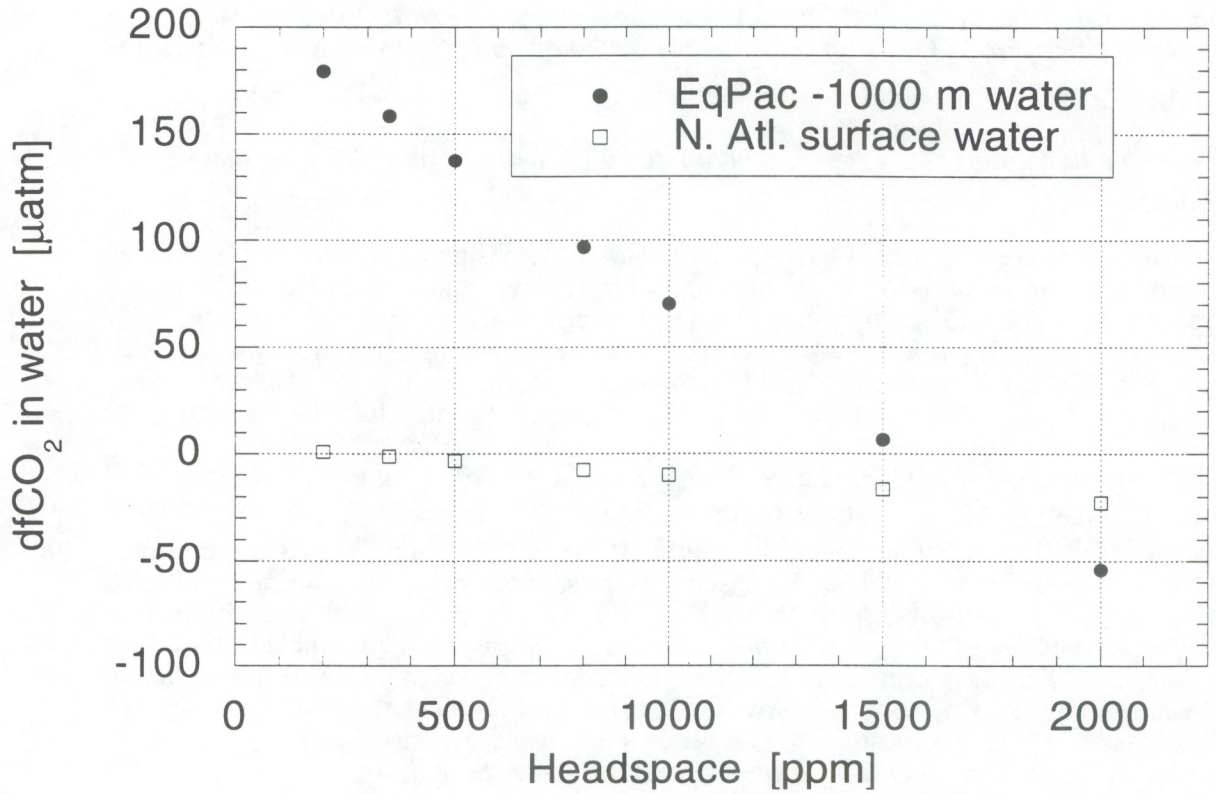

Figure 6. Change in fCO_2 in the water using different displacement gases (= headspace gas). For the EqPac 1000-m water the $fCO_2(20)$ in the water is approximately 1550 µatm and for the N.ATL surface water the $fCO_2(20)$ is about 250 µatm . The difference in sensitivity to choice of displacement gas is because the EqPac 1000-m water is poorly buffered. For the 1000-m water the correction to fCO_2 in the water before equilibration is large if a poor choice of headspace gas is made.

constants are shown in Figures 7 and 8. The carbonate dissociation constants of *Mehrbach et al.*, [1973] are those used extensively by Takahashi [*Takahashi et al.*, 1976][3]. The DOE handbook for inorganic carbon analysis [*DOE*, 1994] recommends the constants of *Roy et al.*, [1993] which are very similar to those obtained by *Goyet and Poisson*, [1989]. This report uses the constants proposed in *Dickson and Millero* [1987]. Figure 7 shows the influence of the different temperature dependence for the constants on the correction of $fCO_2(20)$ to fCO_2 *in situ* along 25 °W during N. ATL-93. The influence of the constants on calculating $fCO_2(20)$ from pH measured at 25 °C and DIC is illustrated in Figure 8 by plotting the percent difference [(measured-calculated)/measured*100] versus fCO_2(measured) for OACES EqPac fall-92. The constants proposed by *Mehrbach et al.*, [1973] and *Roy et al.*, [1993] yield the smallest offset. More importantly, for the discussion below, calculated values differ by as much as 3 % (≈6-10 µatm for surface water and up to 60 µatm for deep water) from the measured values. These differences must be borne in mind in the following sections where the analytical precision of $fCO_2(20)$ measurements are compared with other methods of fCO_2 determination.

Comparison of discrete $fCO_2(20)$ data obtained by IR analyzer and GC from same water sample

A GC based discrete $fCO_2(20)$ system patterned after the design of Neill et al. [1995] was compared with the IR based analyzer on a short cruise from Miami to Puerto Rico during February 1995. The GC based system had a ruthenium catalyst which converted the CO_2 quantitatively into CH_4 which was analyzed in a flame ionization detector. Samples were collected in 120-mL bottles and equilibrated with a 10-mL headspace. The headspace was displaced into a 0.5-mL sample loop and subsequently injected into the detector.

Figure 9 shows the first field comparison of the two systems. The figure is a composite of all samples taken on eleven stations on the "ABACO line" between 72.5 °W and 77 °W along 26.5 °N. The "+" symbols are the results of the GC based analyses and the circles are those of the IR analyses. The GC based system shows more scatter in the composite depth profile. The bottom figure shows the difference in IR analyzer and GC results plotted against $fCO_2(20)$ level. Although the scatter is greater than expected based on the precision of each instruments, much of the scatter is probably due to inexperience with sample processing on the new GC based system. The overall bias for 94 comparisons is +0.7± 2.3 µatm. This test shows an absolute variability range of 0.8 %. Thus within the scatter the two instruments yield the same results.

[3]In this particular excercise the borate constants and borate salinity relationship from *Dickson* [1990] is used instead those of *Lyman*, [1956].

Table 2. Dissociation constants used in calculations:
(note: t = temp in (°C), T= temp in (K))

---

1. In our work (expressed in terms of the seawater hydrogen scale):

K_o : [*Weiss*, 1974; *Weiss and Price*, 1980]:
Exp(-60.2409 + 9345.17/T + 23.3585*Ln(T/100)+S*(0.023517-0.00023656*T + 0.00000047036*T^2))

K_1' : [*Dickson and Millero*, 1987]:
$10^{-(6320.18/T - 126.3405 + 19.568*Ln(T) + (19.894 - 840.39/T-3.0189*Ln(T))*S\text{^}0.5+0.00679*S)}$

K_2' : [*Dickson and Millero*, 1987]:
$10^{-(5143.69/T - 90.1833 + 14.613*Ln(T) + (17.176-690.59/T - 2.6719*Ln(T)*(S)\text{^}0.5 + 0.02169*S)}$

K_b : [*Dickson*, 1990]
Exp(((148.0248 + 137.194*$S^{0.5}$ + 1.62247*S) + (-8966.901 - 2890.51*$S^{0.5}$) - 77.942*S + 1.726*$S^{1.5}$ - 0.0993*S^2)/T+(-24.4344 - 25.085*$S^{0.5}$ - 0.2474*S)*Ln(T) + (0.053105*($S^{0.5}$))*T+Ln(1-S*0.001)))

and

Total Borate (TB)=12.12*S

K_{p2}: [*Kester and Pytkowicz*, 1967]
Exp(-9.039-1450/T)

K_{p3}: [*Kester and Pytkowicz*, 1967]
Exp(4.466-7276/T)

K_{Si}: 4.00E-10

2. In work of Takahashi, (calculations performed using hydrogen activity scale, for details see [*Peng et al.*, 1987])

K_o : [*Weiss*, 1974; *Weiss and Price*, 1980]:
Exp(-60.2409 + 9345.17/T+23.3585*Ln(T/100) + S*(0.023517-0.00023656*T + 0.00000047036*T^2))

K_1' : [*Mehrbach et al.*, 1973]:
$10^{(13.7201 - 0.031334*T-3235.76/T - 0.000013*S*T + 0.1032*(S)\text{^}0.5)}$

K_2' : [*Mehrbach et al.*, 1973]:
$10^{(-5371.9645 - 1.671221*T - 0.22913*S + 128375.28/T + 0.00080944*S*T - 2.136*S/T + (-18.3802*Ln(S) + 2194.3055*Ln(T) + (5617.11/T)*Ln(S))/2.302585)}$

K_b : [*Lyman*, 1956]:
$10^{(-9.26+0.00886*S+0.01*t)}$

and

Total Borate (TB)=410.6*S/35 = 11.73*S

K_{p2}: [*Kester and Pytkowicz*, 1967]
Exp(-9.039-1450/T)

K_{p3}: [*Kester and Pytkowicz*, 1967]
Exp(4.466-7276/T)

K_{Si}: 4.00E-10

Table 2. continued

3. Recommended in DOE handbook (expressed in terms of the "total H^+" scale):

K_0 : [*Weiss*, 1974; *Weiss and Price*, 1980]:

$\text{Exp}(-60.2409 + 9345.17/T + 23.3585*\text{Ln}(T/100) + S*(0.023517 - 0.00023656*T + 0.00000047036*T^2))$

K_1' : [*Roy, et al.*, 1993]:

$\text{Exp}(-2307.1266/T + 2.83655 - 1.5529413*\text{Ln}(T) + (-4.0484/T - 0.20760841)*S^{0.5} + 0.08468345*S - 0.00654208*S^{1.5} + \text{Ln}(1 - 0.001005*S)$

K_2' : [*Roy, et al.*, 1993]:

$\text{Exp}(-3351.6106/T - 9.226508 - 0.2005743*\text{Ln}(T) + (-23.9722/T - 0.10690177)*S^{0.5} + 0.1130822*S - 0.00846934*S^{1.5} + \text{Ln}(1 - 0.001005*S)$

K_b : [*Dickson*, 1993]

$\text{Exp}(((148.0248 + 137.194*S^{0.5} + 1.62247*S) + (-8966.901 - 2890.51*S^{0.5}) - 77.942*S + 1.726*S^{1.5} - 0.0993*S^2)/T + (-24.4344 - 25.085*S^{0.5} - 0.2474*S)*\text{Ln}(T) + (0.053105*(S^{0.5}))*T + \text{Ln}(1 - S*0.001)))$

and

Total Borate (TB)=12.12*S

K_{p2}: [*Millero*, 1974]

$\text{Exp}(-8814.715/T + 172.0883 - 27.927*\text{Ln}(T) + (-160.340/T + 1.3566)*S^{0.5} + (0.37335/T - 0.05778)*S$

K_{p3}: [*Millero*, 1974]

$\text{Exp}(-3070.75/T - 18.141 + (17.27039/T + 2.81197)*S^{0.5} + (-44.99486/T - 0.09984)*S$

K_{Si}: [*Millero*, 1994]

$\text{Exp}(-8904.2/T + 117.385 - 19.334*\text{Ln}(T) + (-458.79/T + 3.5913)*(I/m^o)^{0.5} + (188.74/T - 1.5998)*(I/m^o) + (-12.1652/T + 0.07871)*(I/m^o)^2 + \text{Ln}(1 - 0.001005*S)$

Comparison of underway fCO_2 and discrete fCO_2

The comparison between underway fCO_2 and discrete fCO_2 was performed for the EqPac spring-92 cruise, the EqPac fall-92 cruise, and the N. ATL-93 cruise. The comparison of underway and discrete values for the S. ATL-91 work can be found in Wanninkhof and Thoning [1993]. In each case the discrete values are corrected to SST using the constants listed in Table 2. For the comparison the UW and discrete values were corrected to SST obtained from the CTD, and both the underway and discrete values were normalized to a barometric pressure of 1013.25 mB (= 1 atm). Equilibrator fCO_2 values were corrected to SST using the algorithm of *Weiss et al.*, [1982]. Since the temperature correction generally is smaller than 0.2 °C, the difference in the different correction schemes to correct from equilibrator T to SST for the underway measurements is less than 1 µatm.

The comparison bears out several trends. For EqPac spring-92 underway values are 5.5 ± 4.5 µatm (n=43) higher than the temperature corrected discrete values for fCO_2, ($fCO_{2disc\ situ}$) smaller than 400 µatm. For the twelve comparisons above 400 µatm the underway values are 6.9 ± 5.5 µatm lower (Figure 10). There is no apparent trend with location. The EqPac fall-92 comparison shows underway values which are distinctly lower than the discrete values with the deviation increasing with increasing fCO_2 values

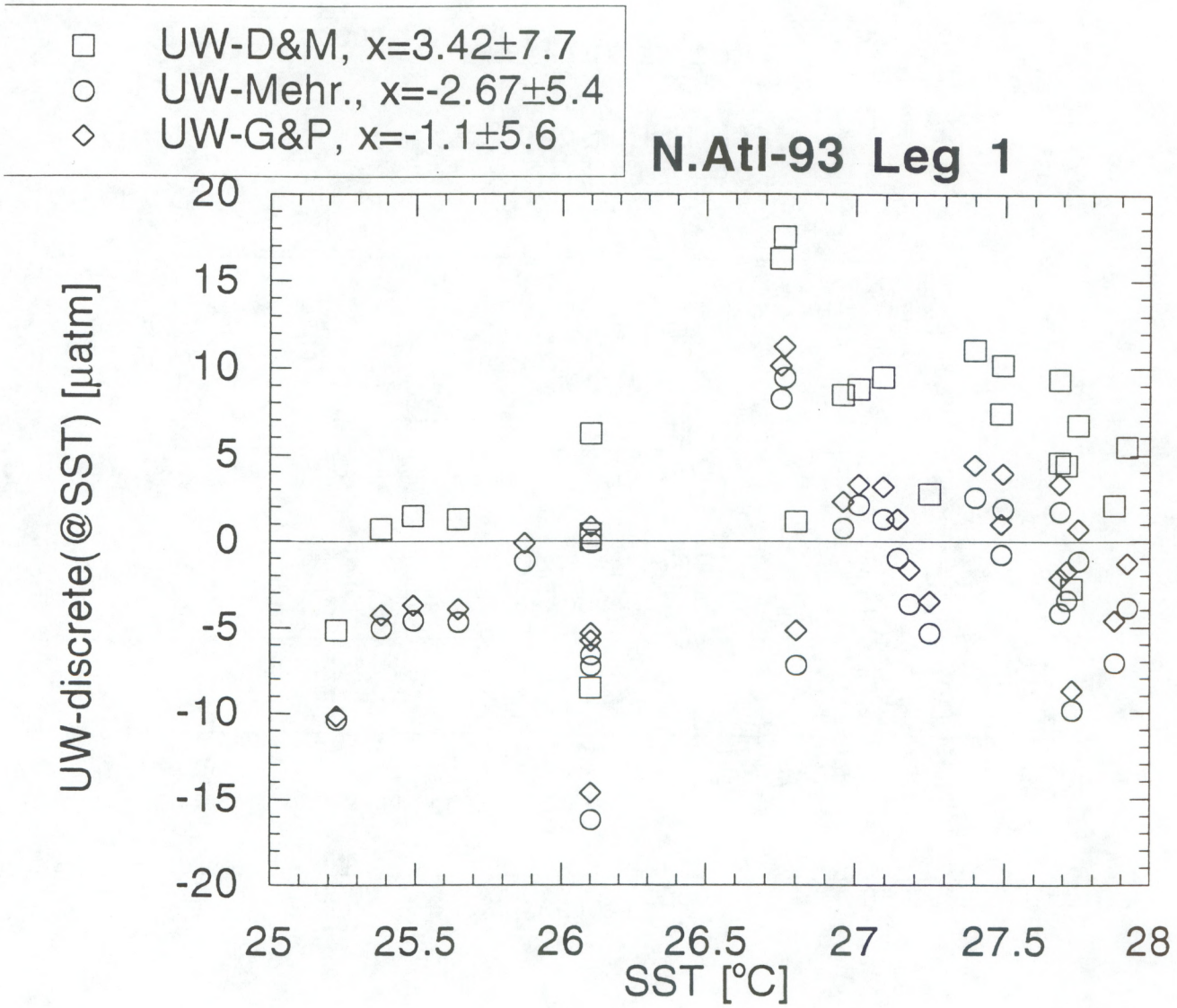

Figure 7. Influence of carbon dissociation constants on temperature correction to convert $fCO_2(20)$ to fCO_2 at SST. The difference between the underway measurements and the temperature corrected discrete fCO_2 values are plotted against temperature for data obtained during the N.ATL-93 cruise, leg 1. D&M=carbon dissociation constants of *Dickson and Millero* [1987]; Mehr.= constants of *Mehrbach* [1973], and G&P= those of *Goyet and Poisson* [1989].

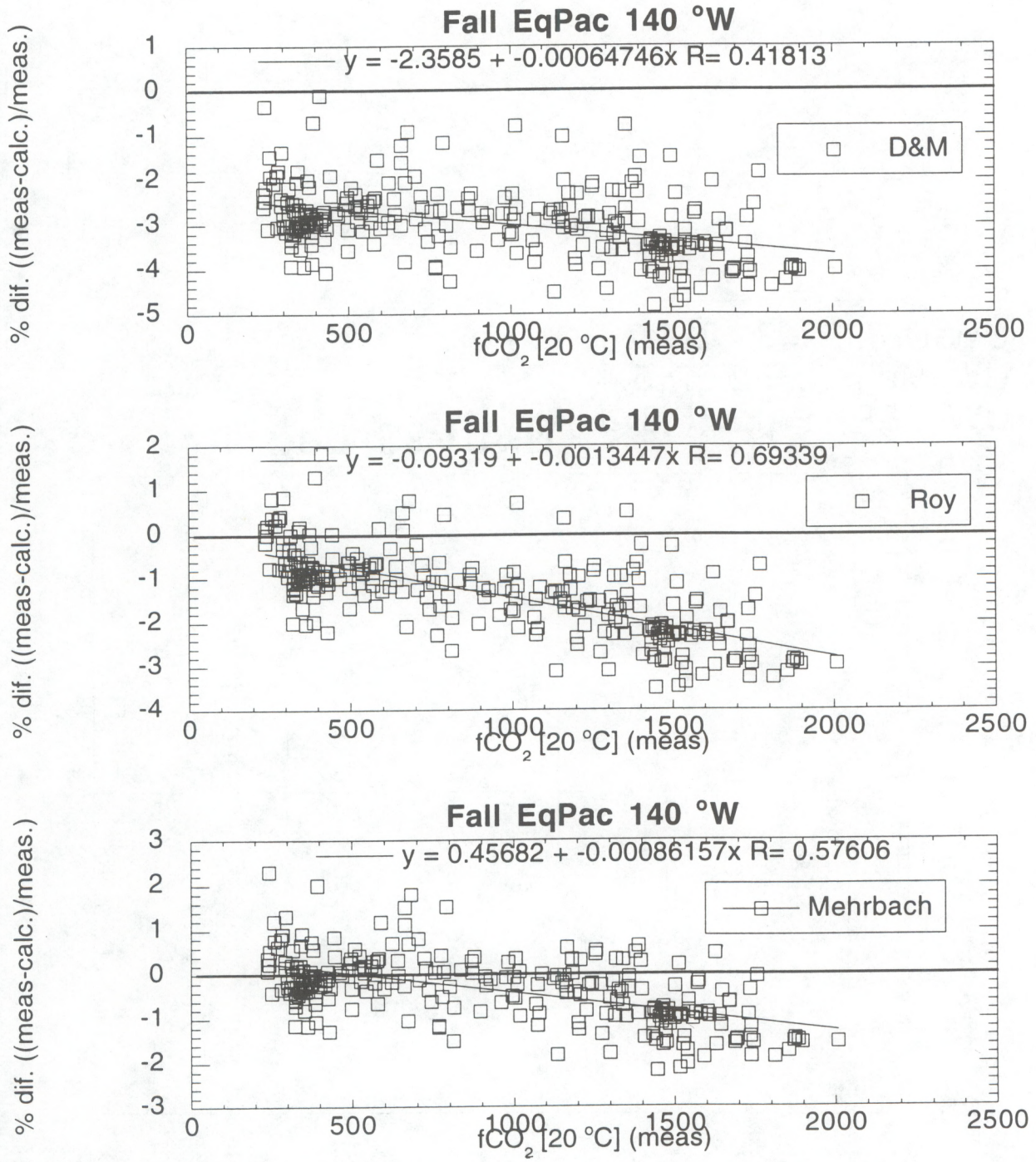

Figure 8. Calculated $fCO_2(20)$ using pH and DIC compared to measured $fCO_2(20)$ for several different sets of dissociation constants. The data was obtained during the EqPac fall-92 cruises. Spectrophotometric pH data is from the group of Dr. R. Byrne of USF.

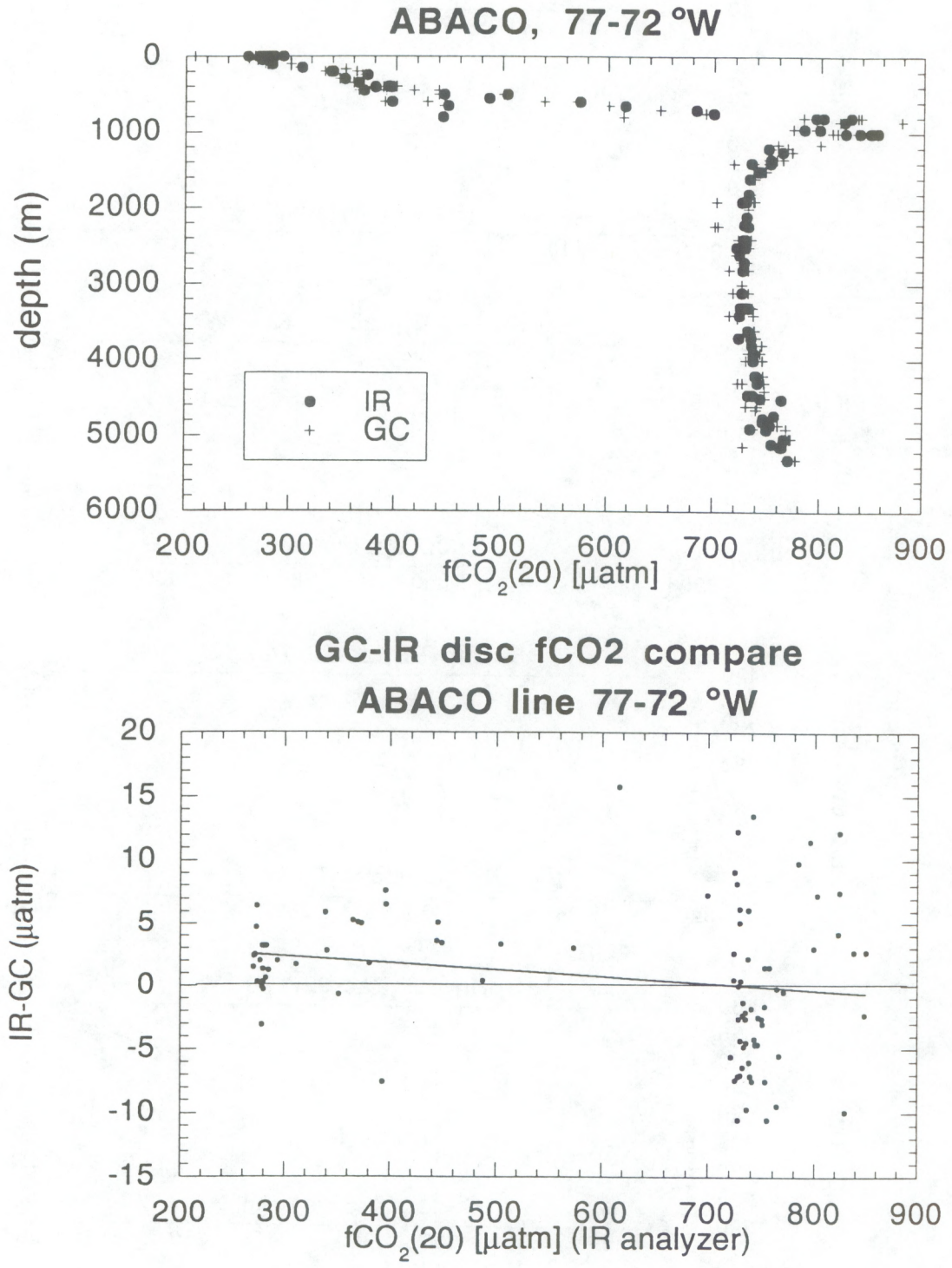

Figure 9. Differences in $fCO_2(20)$ obtained with the IR analyzer system described and a recently fabricated GC based system. Top: a composite plot of all samples taken from 11 stations along the ABACO line (77 °W to 72 °W, 26.5 °N). Bottom: Difference in IR analyzer and GC based measurements from samples taken from the same Niskin™ bottle plotted against $fCO_2(20)$.

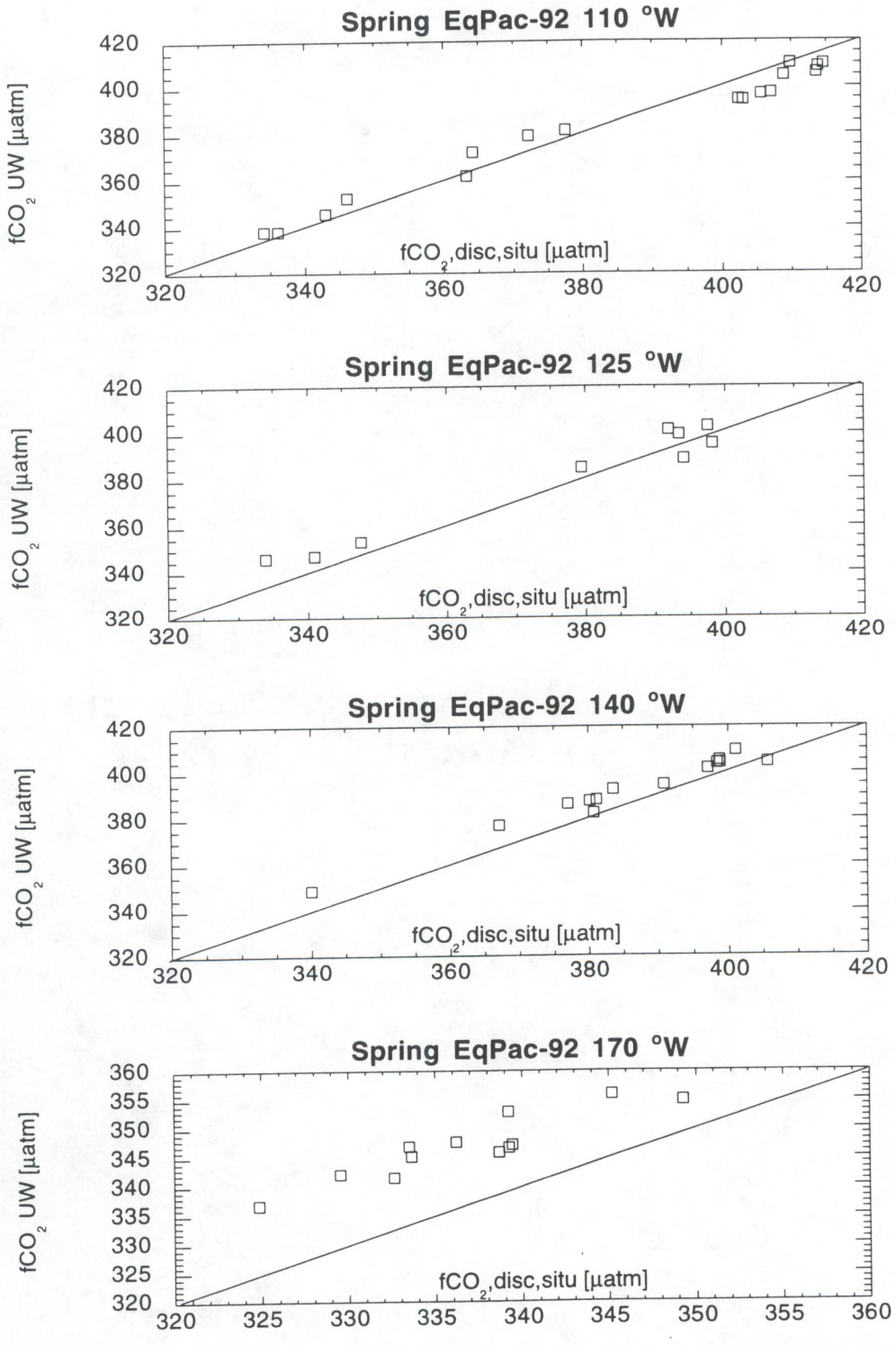

Figure 10. Comparison of the underway fCO_2 measurements with the discrete fCO_2 measurements for surface water during the EqPac spring-92 cruise. The discrete fCO_2 data is corrected to SST using the carbon dissociation constants of *Dickson and Millero* [1987]. For the influence of the dissociation constants on the correction see Figure 7.

(Figure 11). The trend can be well represented by a linear equation applied in the range of observed values:

$fCO_2(UW) = fCO_2(disc) \times 0.899(\pm 0.010) + 36.55\ (\pm 4.31)$ $\qquad r^2=0.995$

The results of the N.ATL-93 comparison is similar to that of EqPac spring-92 with the underway values being slightly higher than the discrete values (Figure 12). The average difference between underway and discrete values is 4.0 ± 5.2 µatm (n=71). There is no apparent trend with location, SST or absolute fCO_2 level. For the N.ATL-93 study the SST between 40 °N and 46 °N was between 19 and 21 °C, and thus the temperature correction will have a small effect on the comparison in this region. For the six stations in this area the difference between UW and discrete values (both corrected to SST) was 3.2± 0.7 µatm. Thus a small bias remains with underway measurements yielding slightly higher values.

For EqPac spring-92 and N. ATL-93, the differences are primarily attributed to the uncertainty in the temperature correction . As shown in Figure 7 the 3.4 µatm offset in the North Atlantic leg 1 data can be reduced to -1.1 µatm if the constants of *Mehrbach* [1973] are used instead of those of *Dickson and Millero* [1987]. The EqPac fall-92 data suggests that the surface seawater was not fully equilibrated in the underway equilibrator possibly because of the high rate of ambient air drawn into the equilibrator either by a leak in the system or because of air loss from the equilibrator through bubbles. This causes greater deviations at higher fCO_2 values, as observed. We do not believe the deviation is caused by uncertainties in the temperature correction as the higher CO_2 values are associated with temperatures closer to 20 °C, that is, the magnitude of the correction should become smaller.

The cause of the bias in the underway system values for EqPac fall-92 appears to be excessive air intake. The headspace of the equilibrator is not recirculated back into the equilibrator after passing through the IR analyzer. This causes a net loss of headspace gas of 50 mL min^{-1} while the headspace is being analyzed (20 minutes each hour). This loss is made up by introduction of ambient air through a vent with intake (mostly) sampling uncontaminated marine air. Because of the large headspace volume (16-L) and rapid response time of the equilibrator (1 to 2 minutes) this should cause a negligible effect.

During the EqPac fall-92 cruises the flow through the equilibrator was 20-30 L min^{-1}. We hypothesize that a significant loss of air from the headspace due to bubble entrainment and subsequent loss of air through the drain. Tests during 1995 indicate an intake through the vents of 0.23 L min^{-1} at a water flow of 15 L min^{-1}; 0.7 L min^{-1} at a water flow of 25 L min^{-1}, and 1.4 L min^{-1} at a water flow of 30 L min^{-1}.

Although no tests were performed during EqPac fall-92, a subsequent test during N. ATL-93 confirmed perturbation of the equilibrator headspace, even at relatively low flow rates. For the tests the rate of air intake through the vent could not be determined because of high variability. But by changing water flow rates, mole fractions in the headspace would vary in the direction expected by ambient air dilution. While on station from 5:00 to 9:00 on 8/15/93 water flow rates were changed from 20 L min^{-1} to 10 L min^{-1} in the sequence listed in Table 3. The 20-minute average mixing ratios in the headspace in Table 3 show a trend consistent with incomplete equilibration.

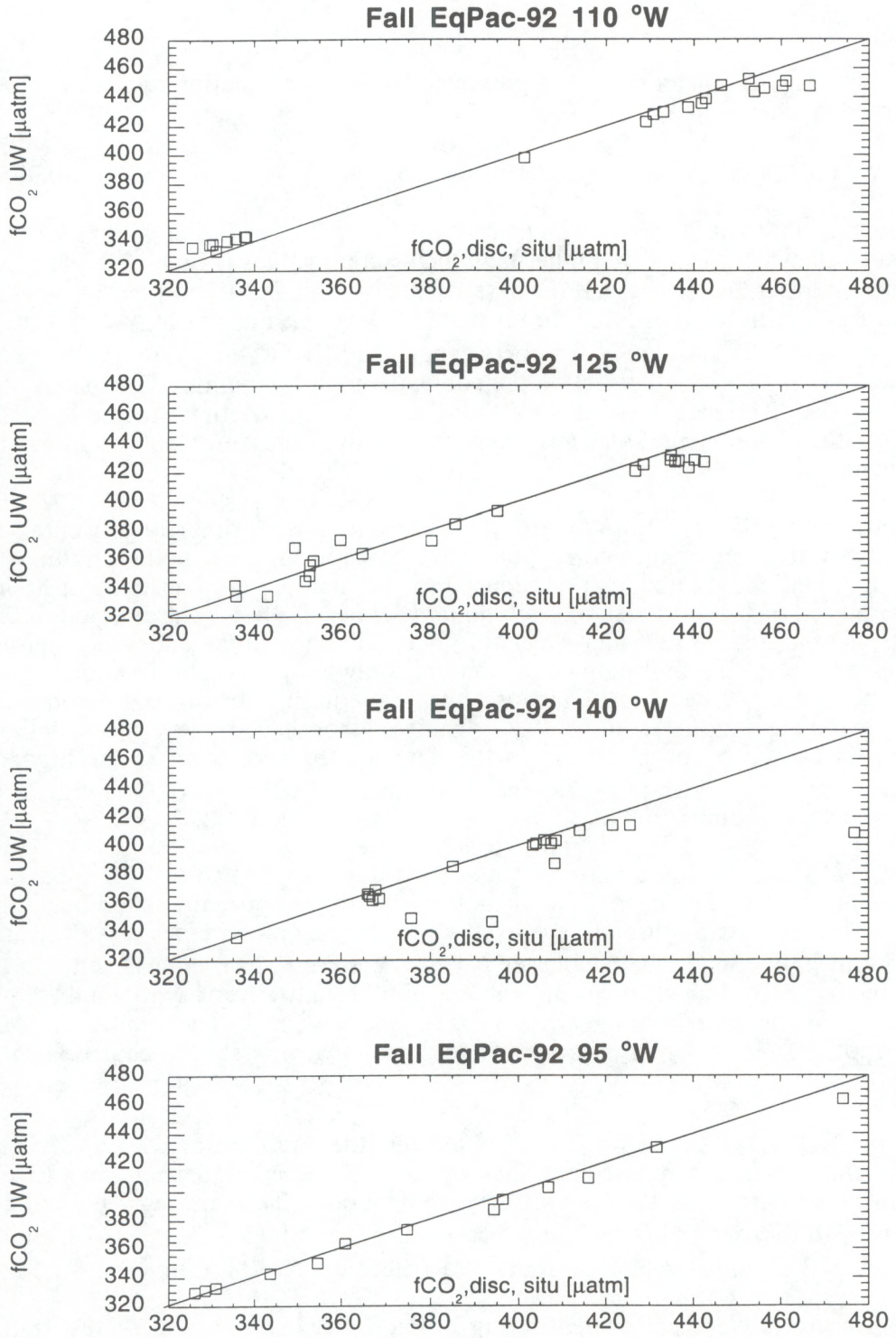

Figure 11. Comparison of the underway fCO_2 measurements with the discrete fCO_2 measurements for surface water during the EqPac fall-92 cruise. The discrete fCO_2 data is corrected to SST using the carbon dissociation constants of *Dickson and Millero* [1987]. The lower values obtained by the underway equilibrator at high fCO_2 are interpreted as incomplete equilibration of the seawater with the headspace.

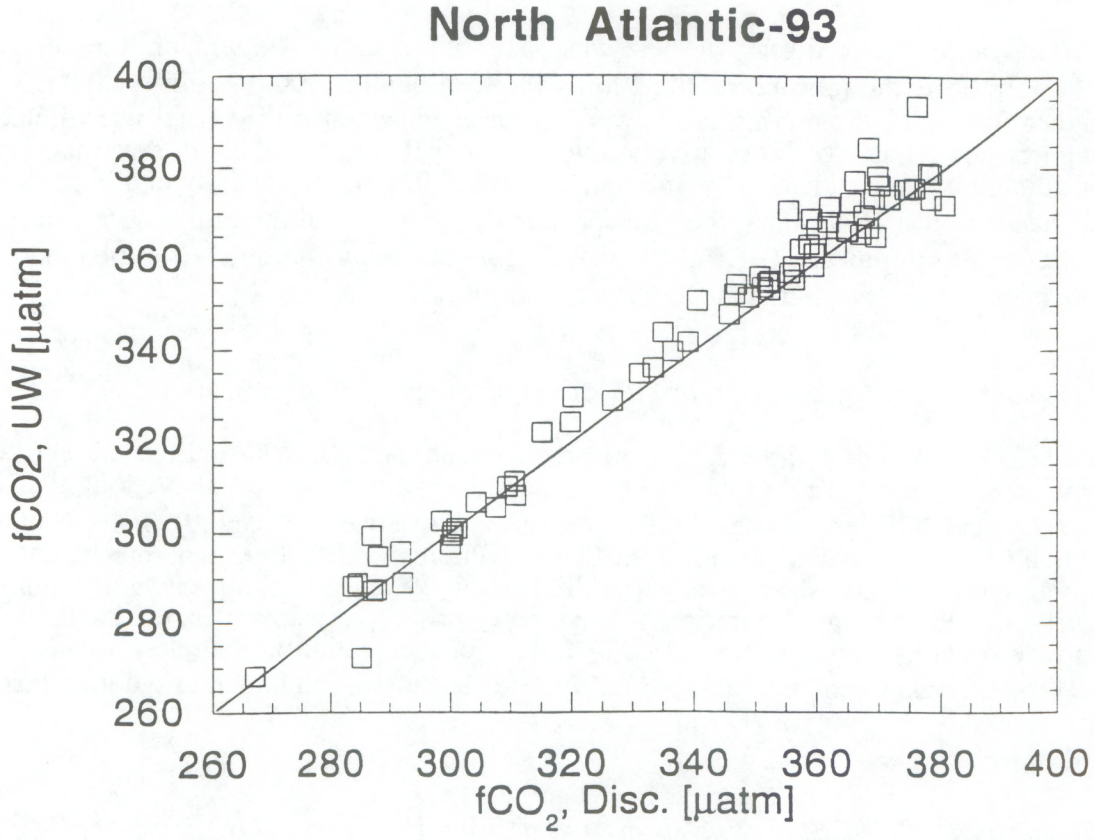

Figure 12. Comparison of the underway fCO_2 measurements with the discrete fCO_2 measurements for surface water during the N.ATL-93 cruise. The discrete fCO_2 data is corrected to SST using the carbon dissociation constants of *Dickson and Millero* [1987]. For the influence of the dissociation constants on the correction see Figure 7.

Table 3. Dependence of headspace mixing ratio on water flow rate

Flow	Mixing ratio	Equil. Temp.	Corr. mixing ratio
20	389.57 ± 0.06	24.05	389.57
15	390.72 ± 0.25	24.05	390.72
10	391.54 ± 0.35	24.09	390.87
15	389.75 ± 0.12	24.04	389.91
20	388.28	24.00	389.10

The air mixing ratio during the test was 351.0 ± 0.2 ppm. The temperature corrected mixing ratio is the ratio normalized to 24.05 °C assuming $dX_{CO2}\ dT^{-1} = 0.0423$. At higher flow rates the mixing ratios were lower as expected if the signal was diluted by ambient air. Thus, even at relatively low flow rates there is a small but systematic trend of dilution of the headspace by ambient air. Assuming the water fully equilibrates with the headspace at 10 L min^{-1}, the headspace reaches 99 % equilibration at 15 L min^{-1} and 96 % equilibration at 20 L min^{-1} water flow rate [equilibration is defined here as: (X_{CO2}water-air) @x L min^{-1} /(X_{CO2}water-air)@10 L min^{-1} * 100].

Comparison of $fCO_2(20)$ discrete with values obtained from other cruises

Two $fCO_2(20)$ inter-comparisons are made between the NOAA/OACES work and work performed by the LDEO group. The comparisons were with data taken along the same transects but at different times. The comparisons are between $pCO_2(20)$[4] values obtained with a GC based system developed at LDEO [Chipman et al., 1993] and our IR analyzer based system. Since short term variability of $fCO_2(20)$ in the upper water column is likely, the comparisons concentrate on property-property, deep water relationships, and surface water by normalization of $fCO_2(20)$ to constant salinity. Samples on our system and the LDEO system are analyzed at 20.00 °C such that no temperature normalizations are necessary.

Comparison of OACES EqPac spring and fall-92 data with JGOFS EqPac TT007 and TT011 data.

Three comparisons are performed for each season along 140 °W from nominally 10 °S to 10 °N:

1. Comparison of salinity normalized $fCO_2(20)$ surface values
2. Comparison of Revelle factors for surface water and water column (the upper 600m)
3. Sub-surface water comparisons for from 5-10 °N, 0 °N, and 5-12 °S versus potential density

[4]The LDEO values are expressed as a partial pressure rather than fugacity. Partial pressures are 0.7 to 1.2 µatm higher than the corresponding fugacity. This small difference is negligible in this comparison, and is not corrected for.

Each comparison suggest small differences, with the IR analyzer based system on average yielding slightly higher values than the GC based system.

Surface water $fCO_2(20)$ comparisons should be done with caution because of large and rapid variations due to changes in upwelling rates and lateral movement of water by tropical instability waves (TIW). The time during which the cruises were performed are as follows:

TT007 JGOFS EqPac	2/3 to 3/9/92
OACES EqPac spring-92, 140 °W	4/24 to 5/5/92
TT011 JGOFS EqPac	8/5 to 9/18/92
OACES EqPac fall-92, 140 °W	9/10 to 9/18/92

The mixed layer values are plotted versus latitude in Figure 13 . For most locations the LDEO values are 5 to 10 µatm lower. Notable exceptions are the mixed layer values in the fall from 0 to 2 °N where the LDEO values are significantly higher. These high values correspond with lower SST and higher nitrate salinity indicative of recently upwelled water possibly by means of a TIW. A more robust comparison can be made plotting the $fCO_2(20),35$ ($fCO_2(20)$ normalized to Salinity = 35) versus density (Figure 14). $fCO_2(20),35$ is defined as [*Archer et al.*, 1995]:

$$fCO_2(20),35 = fCO_2(20),S * (35/S)^n$$

where $$n = 1.15-[6.45*10^{-4}*fCO_2(20),S]$$

For the spring there is no strong trend of $fCO_2(20)$ with density with low $fCO_2(20)$ values at both high and low density. The LDEO values generally fall below the OACES values. During the fall under more vigorous upwelling, $fCO_2(20)$ increases near linearly with potential density for values greater than 21.7. LDEO values fall below the OACES fCO_2 values up to densities of 23.5.

Figure 15 shows a plot of ln ($fCO_2(20),35$) versus ln (DIC,35) in the mixed layer for both spring and fall. (DIC,35) is DIC normalized to a salinity of 35. The slope of the trend is the Revelle factor ($Re = [d(\ln(pCO2)\ \{d(\ln(DIC))\}^{-1}]_{S,T,\ TAlk}$). For the spring the Revelle factors are 7.5 and 9.2 for the LDEO[5] and OACES cruises, respectively. For the fall the values are 9.4 and 8.8 for the two cruises. Figure 15 shows that the OACES fCO_2 values are systematically higher when plotted against DIC,35. The difference in the spring is in part caused by higher measured DIC,35 values during the TT007 cruise particularly in the southern hemisphere (Figure 16).

$fCO_2(20)$ vs. DIC trends are shown as ln ($fCO_2(20),35$) versus ln (DIC, 35) in Figure 17. The near-quadratic increase with depth breaks down at high DIC values due to

[5]In *Archer at al.* [1995] the LDEO Revelle factors were reported as 7.9 ± 0.5 for the spring and 9.3 ± 0.1 in the fall. The small difference is likely caused by different rejection criteria for the data used in the analysis.

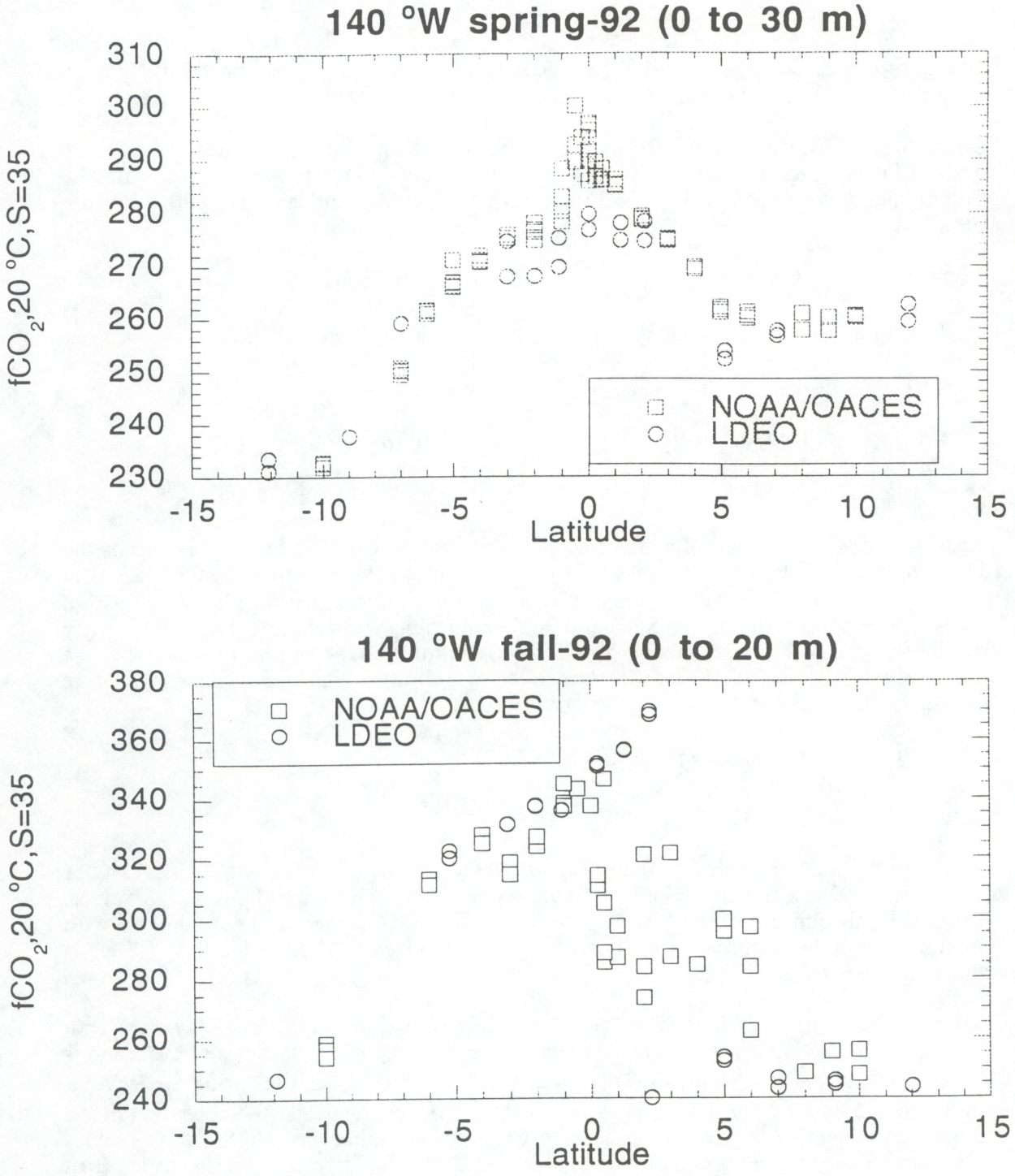

Figure 13. Comparison of EqPac spring and fall-92 surface water $fCO_2(20)$ normalized to S=35 with $fCO_2(20)$ obtained along the same (140 °W) transect by LDEO during the same season and year but about 1.5 months earlier for the (boreal) spring and 2 weeks later for the fall.

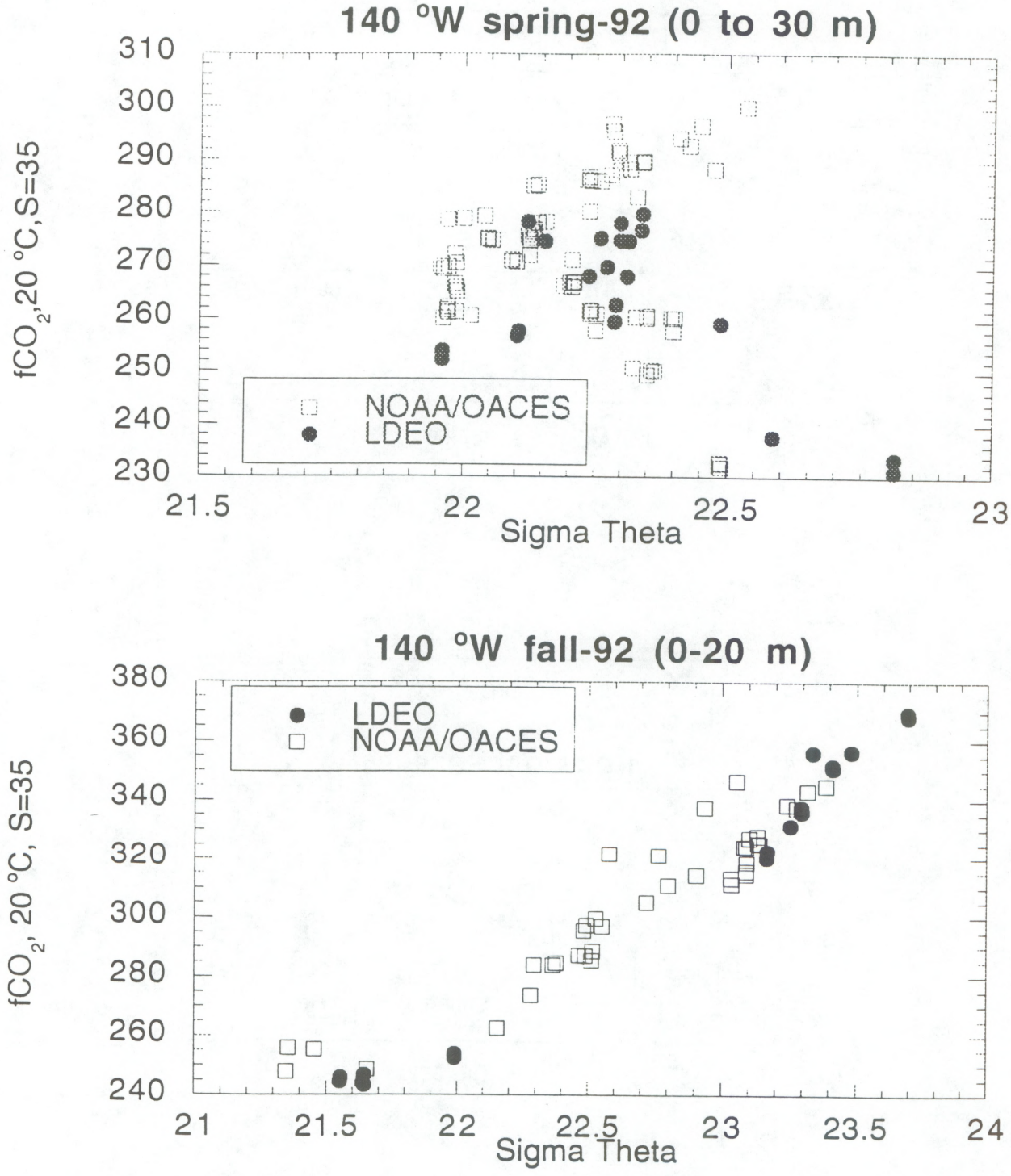

Figure 14. Comparison of EqPac spring and fall-92 surface water $fCO_2(20)$ normalized to S=35 with $fCO_2(20)$ obtained along the same (140 °W) transect by LDEO during the same season and year. The surface water data is plotted against potential density.

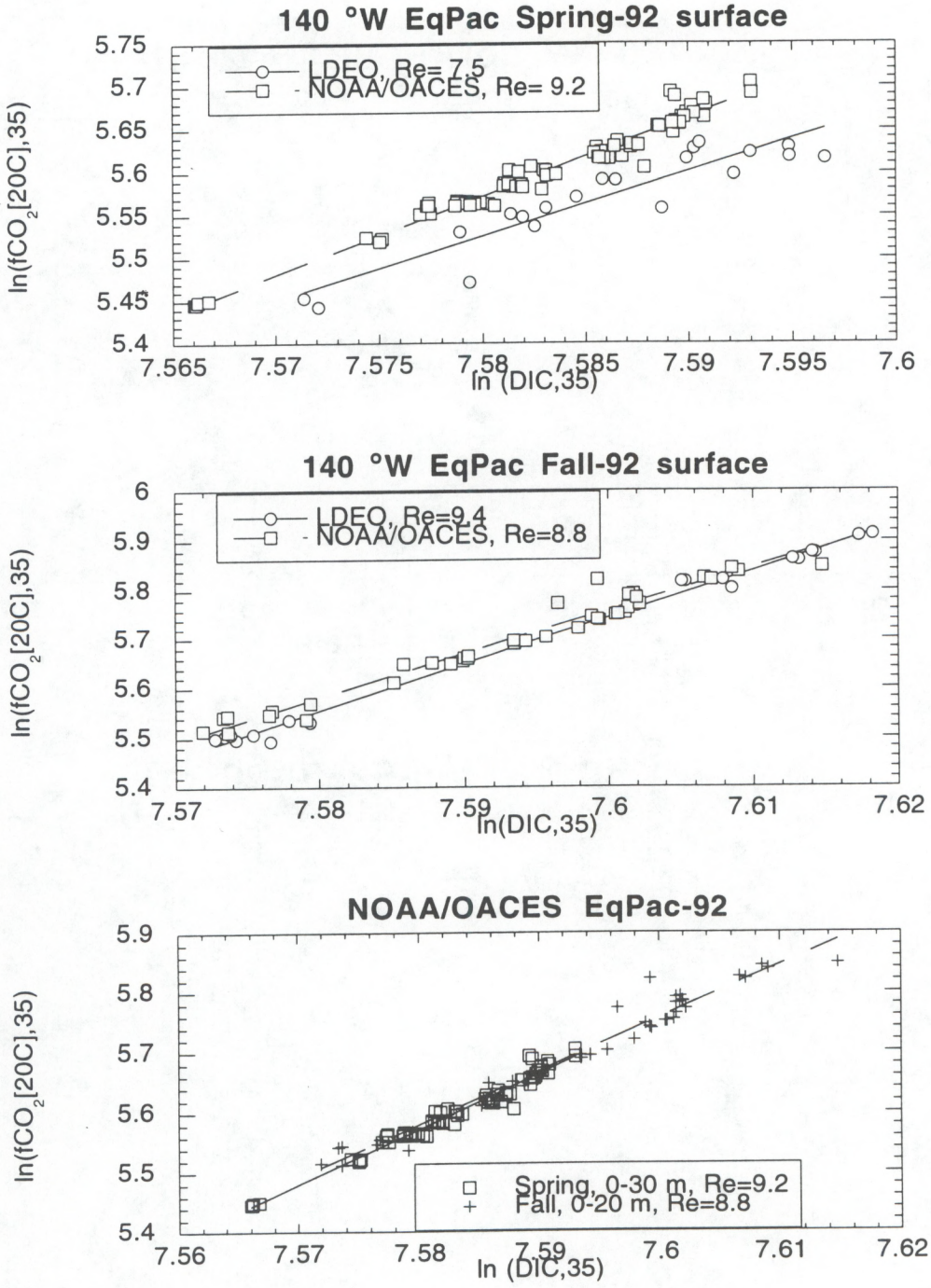

Figure 15. The natural log of $fCO_2(20)$ [$\ln(fCO_2(20))$] normalized to S=35 plotted against the natural log if salinity normalized DIC [ln (DIC)] for the OACES and LDEO results during EqPac spring and fall-92. The slope of the lines gives the Revelle (or buffering) factor of the oceanic carbonate system, [Re = $d(\ln(pCO2)\ \{d(\ln(DIC))\}^{-1}{}_{S,TAlk}$]. The bottom panel suggests that there is no systematic difference between the spring and fall OACES results.

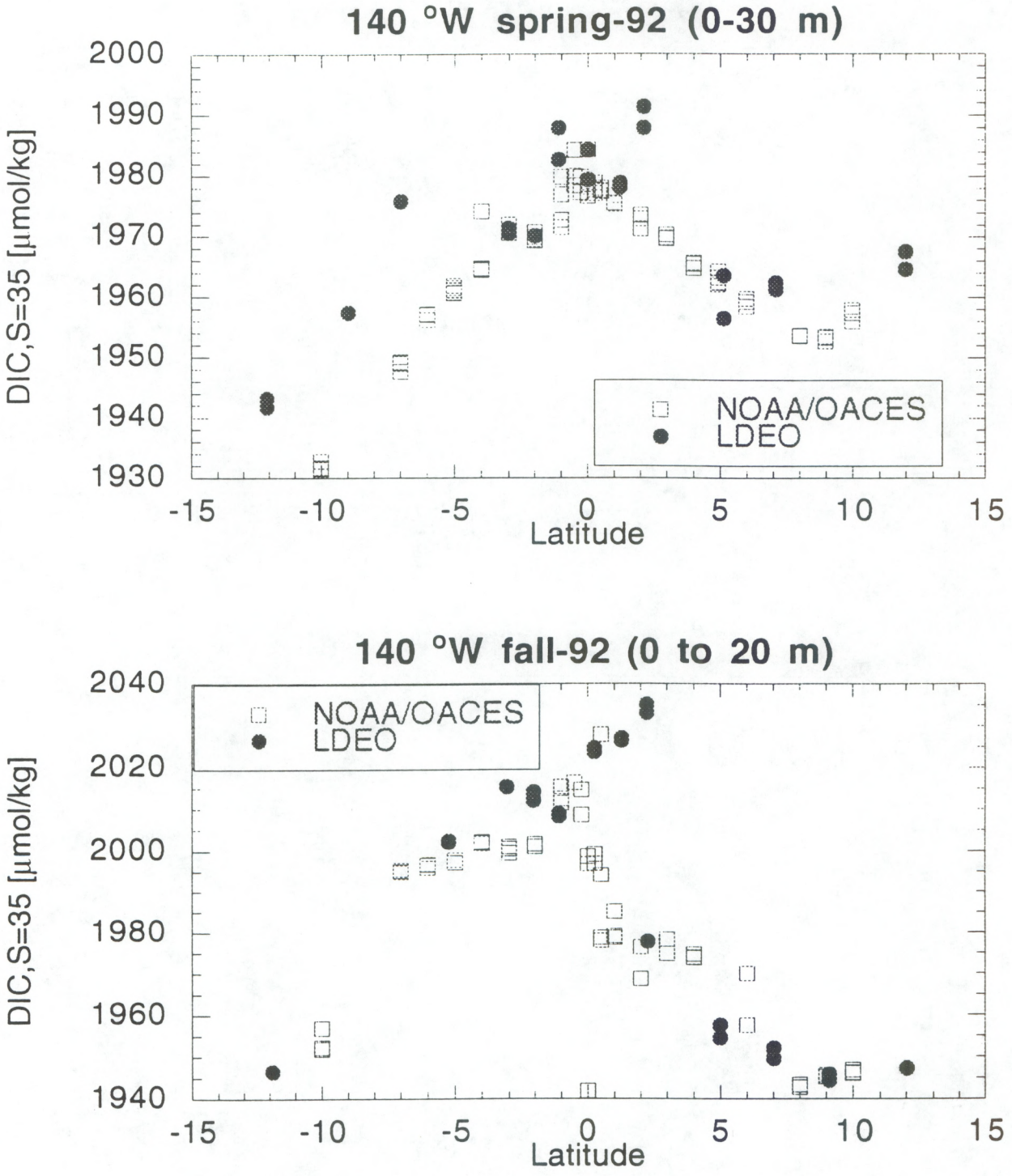

Figure 16. Comparison of surface DIC values normalized to S=35 (DIC,35) for EqPac spring and fall-92 along 140 °W for the OACES and LDEO work.

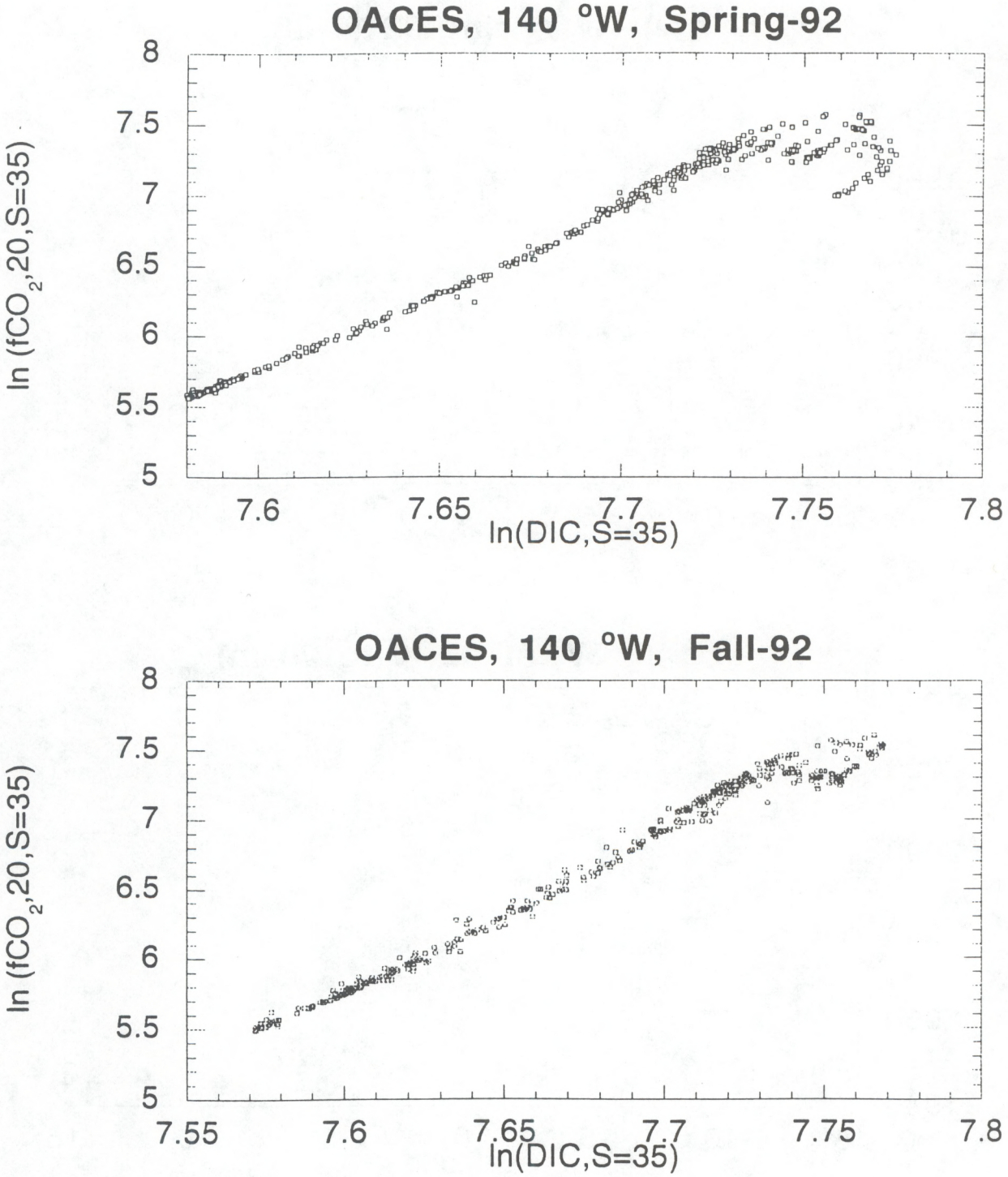

Figure 17. EqPac spring and fall-92 water column (top 1000 m) ln(fCO_2(20)) normalized to S=35 plotted against salinity normalized ln (DIC). The slope of the trend gives the Revelle (or buffering) factor of the oceanic carbonate system.

dissolution of calcium carbonate which depresses the $fCO_2(20)$ values. The Revelle factor shown in Figure 18 is determined from the slope in Figure 17 for DIC,35 values up to 2275 μmol kg^{-1} [ln (DIC, 35)=7.73]. The slope of the Revelle factor versus ln (DIC, 35) for the spring is significantly different between the OACES and LDEO study (44.2 for the OACES work and 38.8 for the LDEO results); for the fall slightly better agreement is observed with slopes of 47.1 for the OACES work and 43.43 for the LDEO results (Figure 18).

It is difficult to determine the magnitude of possible biases in sub-surface $fCO_2(20)$ values between the datasets since sample location differed and variability is large. Plots of $fCO_2(20)$ vs. potential density, DIC vs. potential density, and DIC vs. $fCO_2(20)$ for latitude ranges from 5 °N to 9 (or 10) °N and 5 °S to 10 (or 12) °S along 140 °W in the thermocline (potential density > 25) are presented in Figures 19 through 22. Since the surface waters of the Equatorial Pacific exhibit large variability no clear trends are apparent. From 5 °N to 9 °N region during EqPac spring-92 the $fCO_2(20)$ values plotted against DIC for LDEO lie below the OACES trend by as much as 100 μatm. This appears to be an offset in $fCO_2(20)$ rather than DIC since no systematic DIC differences are observed between the DIC data plotted versus potential density (Figure 19). Not enough comparable data is available for the southern hemisphere (5 °S to 12 °S) in the spring to draw any conclusions for this region.

In contrast, the OACES and LDEO values in the fall show better agreement (Figures 21 and 22). The data in the northern hemisphere show similar $fCO_2(20)$ values and similar DIC values for OACES and LDEO when plotted against potential density. The $fCO_2(20)$ vs. DIC plot shows the LDEO values falling in line with the OACES data.

Deeper casts were performed during the OACES and JGOFS cruises at the Equator (3500 dB and 2000 dB, respectively) in the spring. $fCO_2(20)$, DIC, and total alkalinity (TAlk) are plotted versus density in Figure 23. Again, the comparison shows biases, even in the potential density range of 26.5 to 28 (300 to 2000 dB). It is unlikely that the differences are real but in this energetic region it cannot be discounted. In this comparison the LDEO and OACES $fCO_2(20)$ values show reasonable agreement but the DIC and TAlk values obtained on the OACES cruises are about 10 μmol kg^{-1} (μEq kg^{-1}) lower.

In summary, surface $fCO_2(20)$ values of LDEO appear systematically lower by 5 to 10 μatm than the discrete values obtained during the NOAA/OACES EqPac cruises. Surface and subsurface Revelle factors are very similar between LDEO and the OACES work for the fall. The spring values show significant differences. The Revelle factor for surface values of LDEO are lower than those of OACES and the trend with increasing DIC is weaker. There is inconclusive evidence that the LDEO subsurface $fCO_2(20)$ values are lower as well. Poor correlations of DIC values preclude a definite answer if this difference is natural variability or instrument bias.

Comparison of OACES S.ATL-91 with SAVE leg 5/HYDROS leg 4

The SAVE/HYDROS and S.ATL-91 cruises took place two years apart during different seasons but yield a good opportunity to compare discrete fCO_2 data because of extensive sampling of deep water. This water should undergo little chemical change over this time period. The following cruise segments were compared:

Save 5:	Stations 237-256,	33 °S, 25 °W to 42 °S, 28 °W,	February 89
Hydros 4:	Stations 314-373,	33 °S, 25 °W to 1 °N, 25 °W ,	March 89

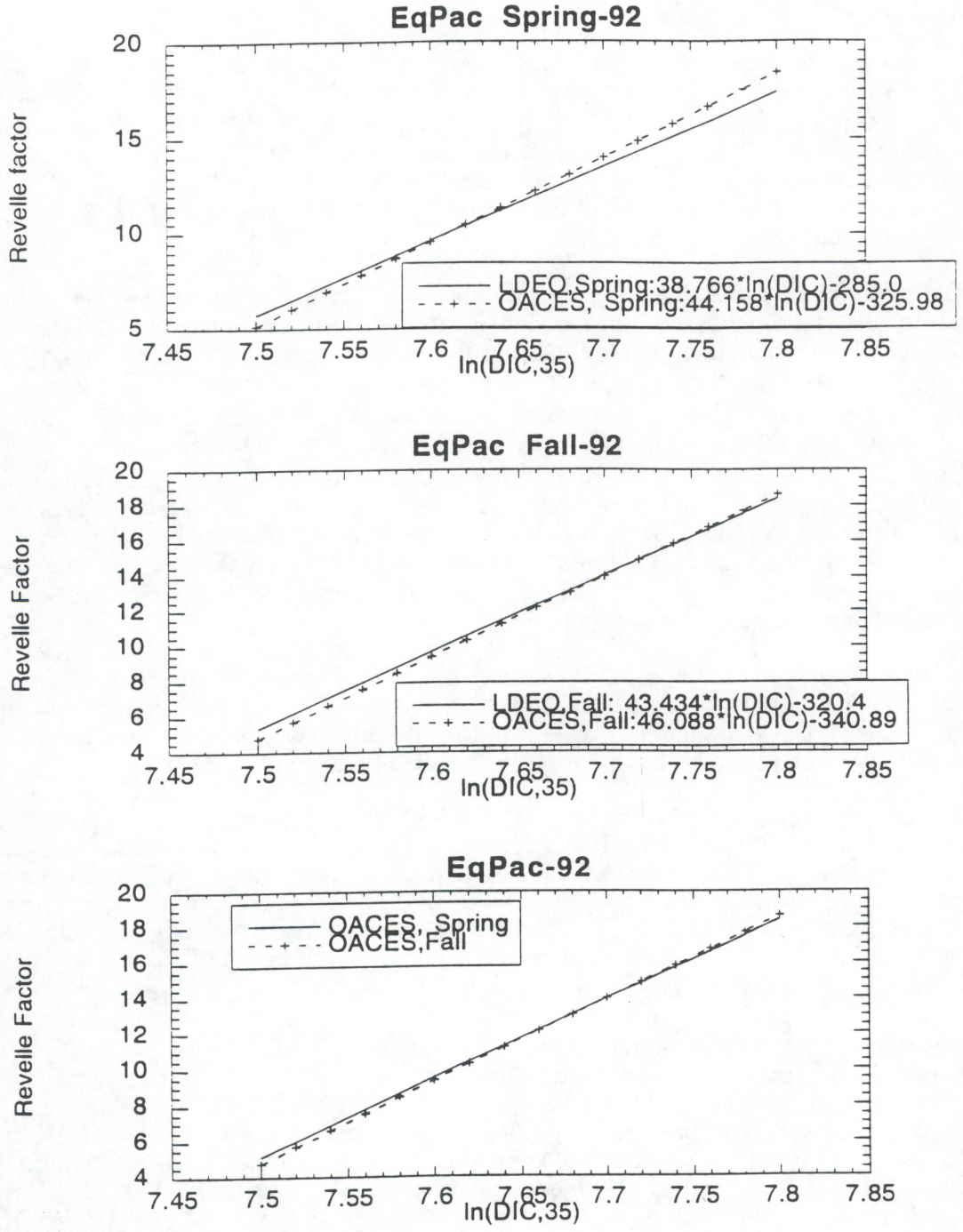

Figure 18. Revelle factor vs. ln DIC,35 for LDEO and OACES work during EqPac spring and fall-92. The Revelle factor was determined from the first differential of the slope of the data in Figure 17 up to ln (DIC,35) of 7.7 (or DIC,35 of 2210 μmol kg^{-1}).

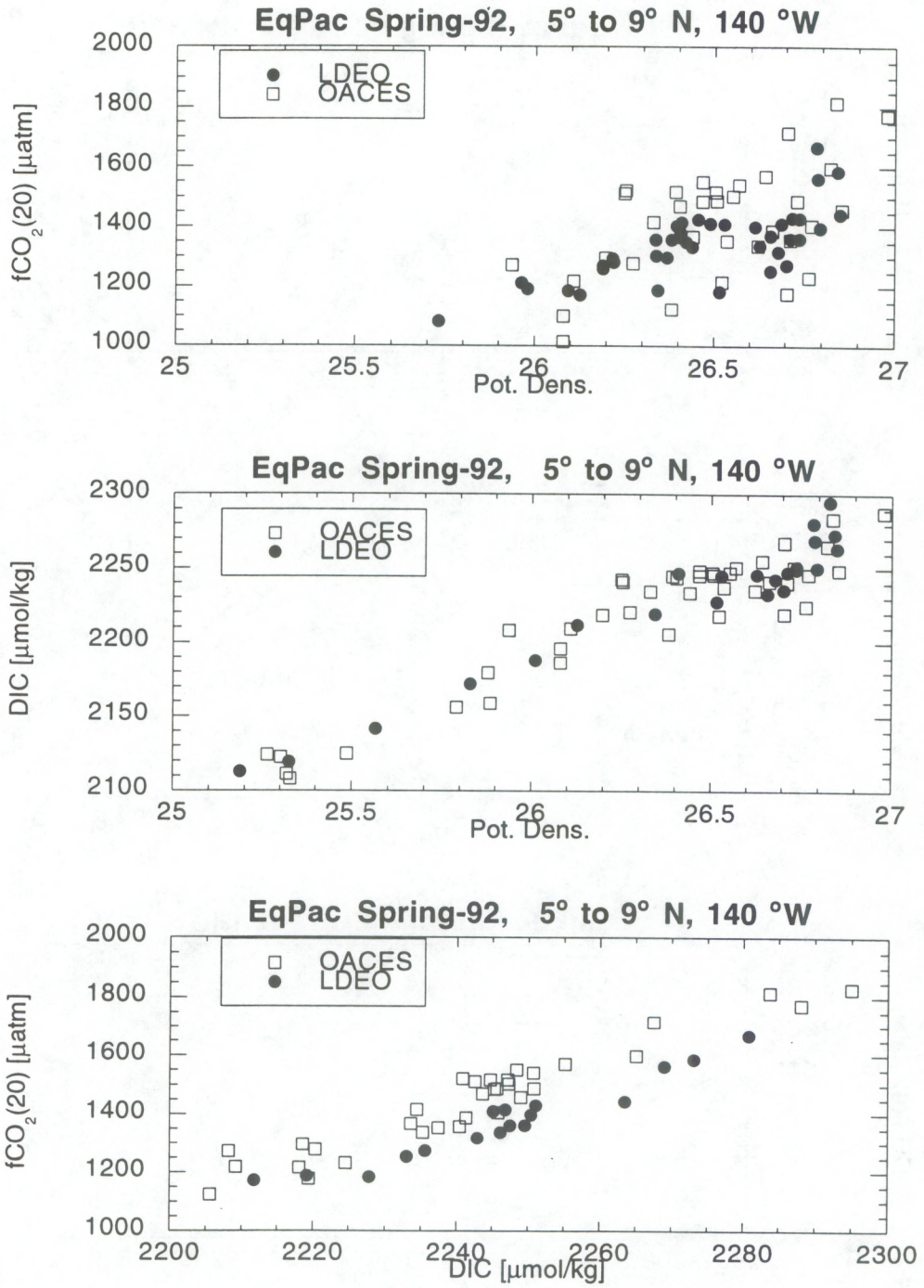

Figure 19. $fCO_2(20)$ vs. pot. dens. (top); DIC vs. pot. dens. (middle); and $fCO_2(20)$ vs. DIC, 35 (bottom) for thermocline water from 100 to 1000 m from 5 to 9 °N, 140 °W, EqPac spring-92.

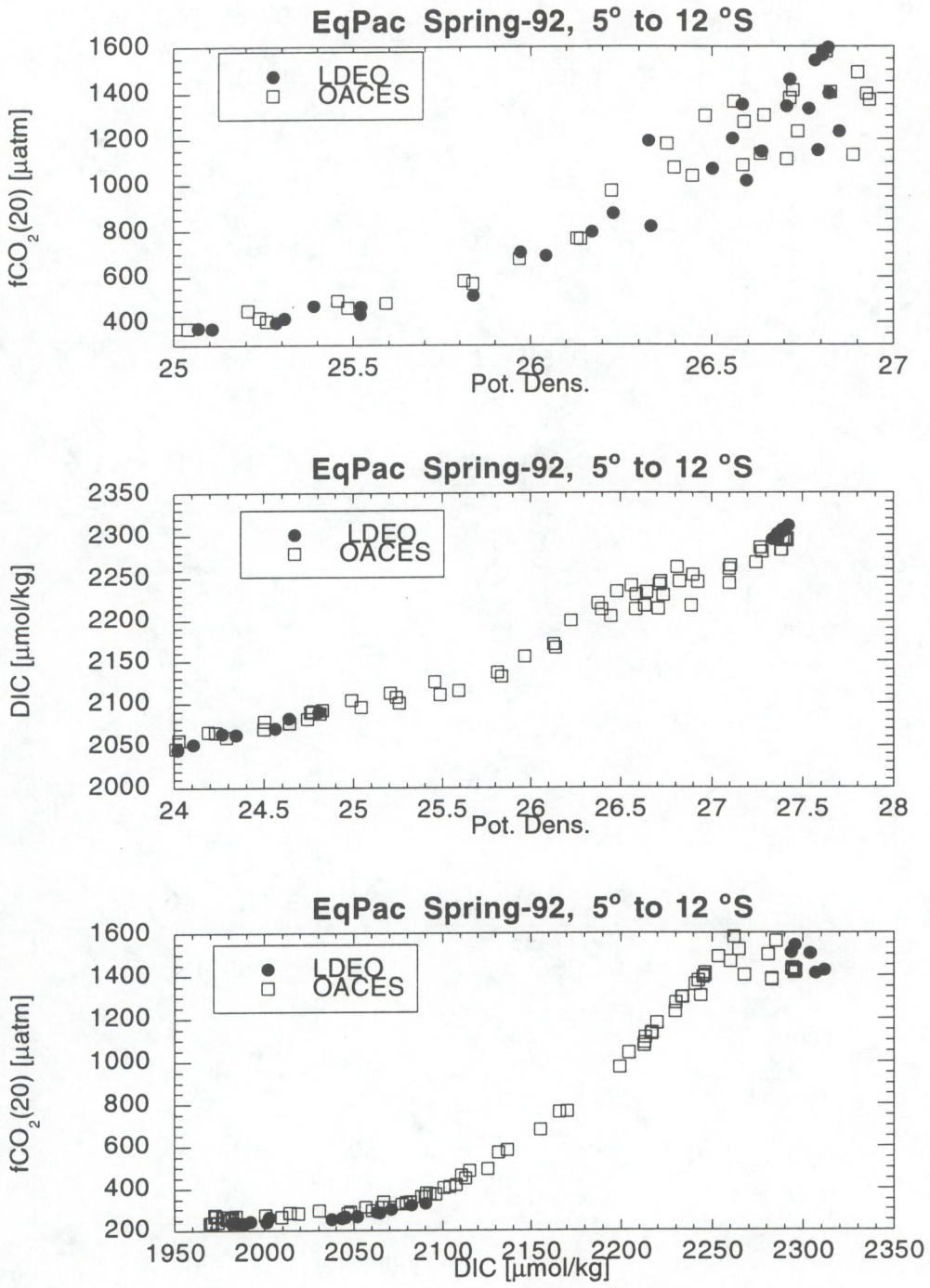

Figure 20. $fCO_2(20)$ vs. pot. dens. (top); DIC vs. pot. dens. (middle); and $fCO_2(20)$ vs. DIC, 35 (bottom) for thermocline water from 100 to 1000 m from 5 to 12 °S, 140 °W, EqPac spring-92.

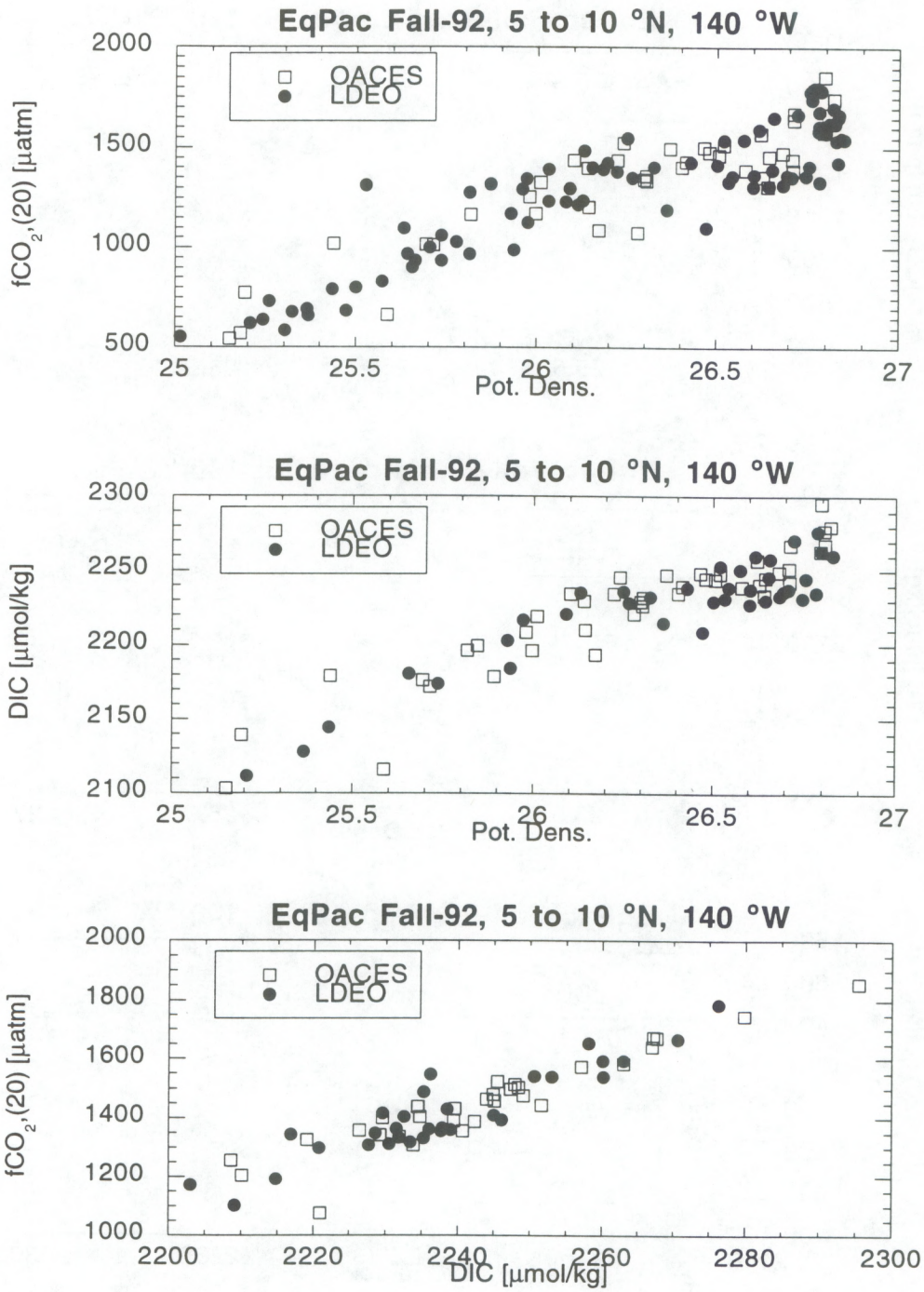

Figure 21. $fCO_2(20)$ vs. pot. dens. (top); DIC vs. pot. dens. (middle); and $fCO_2(20)$ vs. DIC, 35 (bottom) for thermocline water from 100 to 1000 m from 5 to 9 °N, 140 °W, EqPac fall-92.

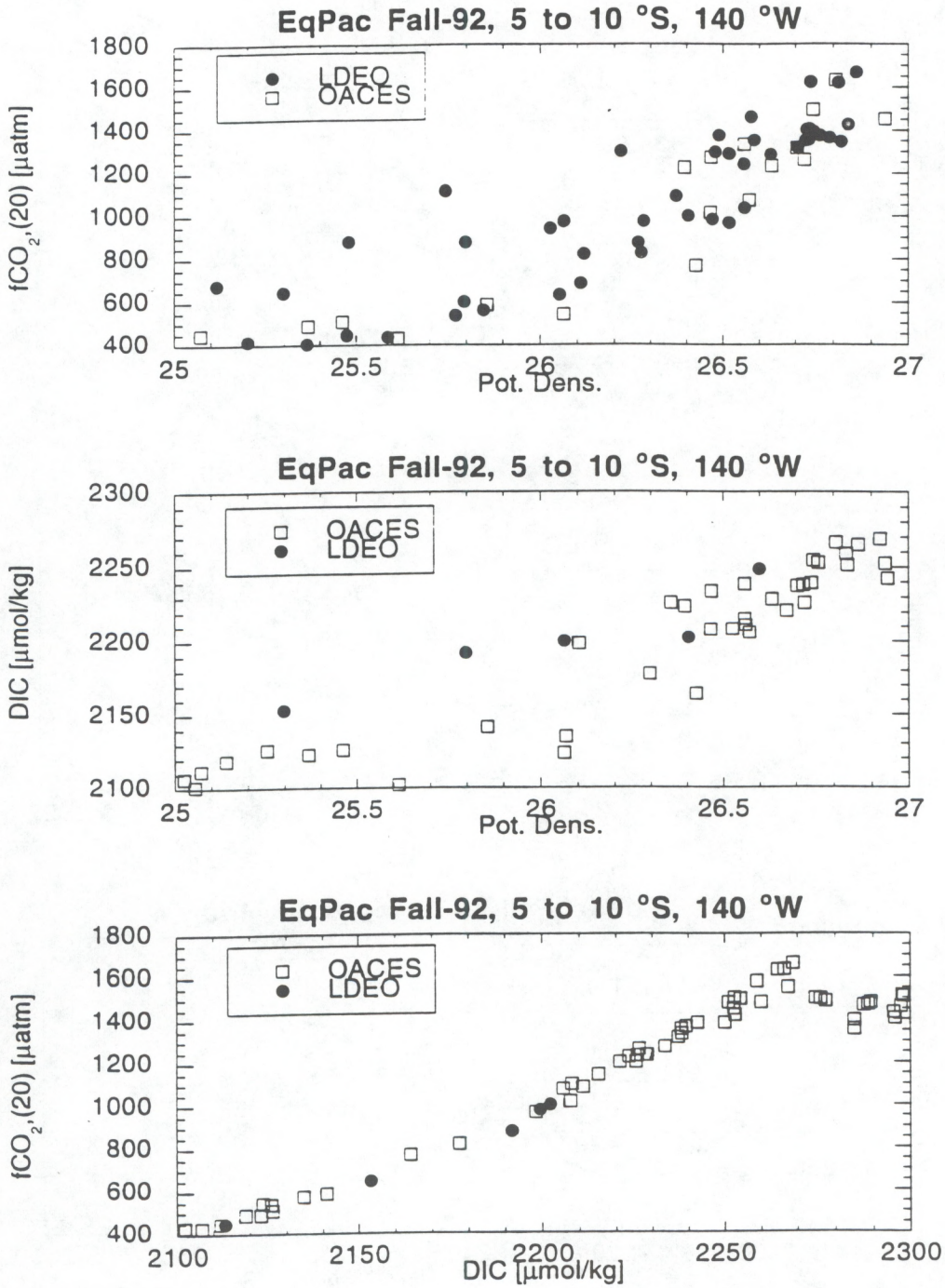

Figure 22. $fCO_2(20)$ vs. pot. dens. (top); DIC vs. pot. dens. (middle); and $fCO_2(20)$ vs. DIC, 35 (bottom) for thermocline water from 100-1000 m from 5 to 10 °S, 140 °W, EqPac fall-92.

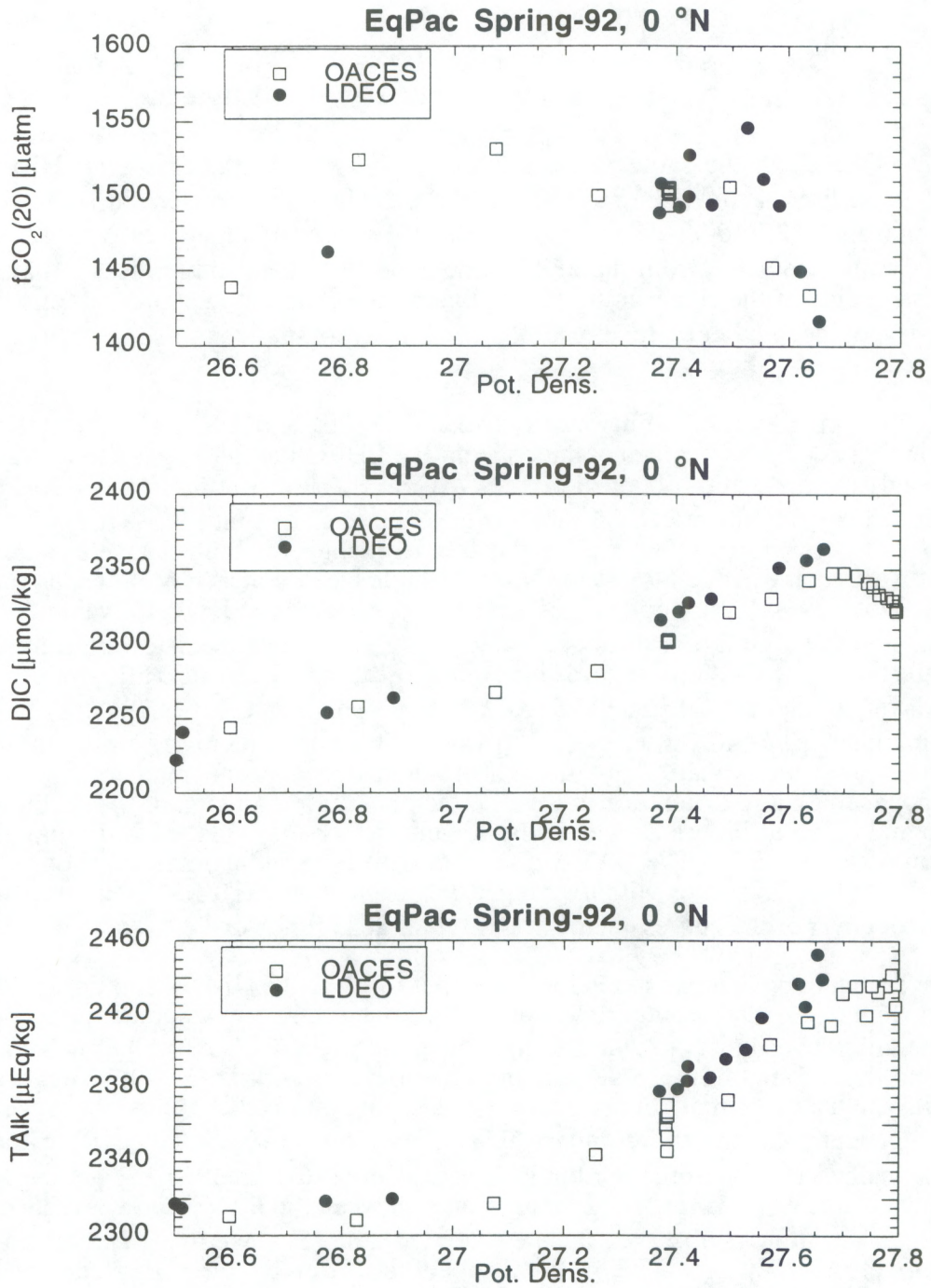

Figure 23. $fCO_2(20)$ vs. pot. dens. (top); DIC vs. pot. dens. (middle); and TAlk vs. pot. dens. for intermediate water at 0 °N, 140 °W, EqPac spring-92.

with:

S.ATL-91: Stations 7-31, 1 °N, 25 °W to 42 °S, 32 °W, July 91

From 1 °N to 27 °S the same cruise track was followed for the SAVE/HYDROS and S.ATL-91 cruises. From 27 °S to 32 °S, the S.ATL-91 cruise went in southwesterly direction from 25 °W to 32 °W and then proceeded southward along 32 °W to 42 °S. The SAVE-5 cruise deviated from the 25 °W line at 33 °S. Since both cruises remained on the western side of the ridge in the Brazil Basin no significant lateral variations in CO_2 chemistry of deep water are expected, such that comparisons down to 42 °S are warranted.

Figure 24 compares the salinity normalized $fCO_2(20)$ and DIC values plotted on a logarithmic scale for the values obtained from the LDEO group (referred to as SAVE in the legend) and the values obtained on the OACES, S.ATL-91 cruise (OACES-91). The comparison is made for a DIC,35 range from 1930 to 2143 µmol kg^{-1} ($fCO_2(20)$,35 of 250 to 740 µatm). At higher values the trends change for both datasets because of distinctly different Revelle factors for North Atlantic Deep Water (NADW) and Antarctic Bottom Water (AABW). Good correspondence is observed at low DIC values of 1930 µmol kg^{-1} and at high DIC values of 2140 µmol kg^{-1}. For intermediate values the SAVE data falls below the OACES trend. This is in part caused by low $fCO_2(20)$ values in the mixed layer during SAVE from 38 °S to 42 °S corresponding to DIC,35 values of 2040 to 2060 µmol kg^{-1} [(ln(DIC,35) from 7.62 to 7.63)]. A second-order polynomial fit through the data shows this deviation. Although the deviation appears small in Figure 24, it corresponds to a large difference in Revelle factors. Differentiation of the second-order polynomial curve in Figure 24 yields the Revelle factor. It is plotted in Figure 25 as a function of ln(DIC,35). The SAVE data appear to have an anomalously low Revelle factor at low DIC,35 values with a stronger dependency on ln(DIC,35) than the OACES data. Cross over of the curves occurs at DIC,35 of 2035 µmol kg^{-1}.

A more encouraging comparison is for that of $fCO_2(20)$ in the NADW and upper AABW. Figures 26 and 27 show comparisons of $fCO_2(20)$ and DIC versus potential density for six locations between 0 °N to 29.5 °S. Agreement between $fCO_2(20)$ values is better than 1 %, and deviations often are systematically correlated with DIC. This suggests real variability in the water mass either because of slightly different locations or changes with time. For example, for the comparison at 11 °S the OACES $fCO_2(20)$ values are systematically 5 to 10 µatm lower but DIC values are 2 to 4 µmol kg^{-1} lower suggesting that much of the trend is real rather than a bias between the SAVE and OACES results. The largest deviation is observed for the station at 29.5 °S where $fCO_2(20)$ values differ by as much as 20 µatm. The stations locations differ by three degrees longitude suggesting that this might be caused by spatial and temporal variability. For this southern station mixing of water from northern origin with Antarctic water can have a pronounced influence on the carbon chemistry. Although the comparison can hardly be called robust, the good agreement of the $fCO_2(20)$ values in the NADW is an encouraging sign that there are no large biases in the datasets at intermediate (700-800 µatm) fCO_2 (20) levels.

Comparison with $fCO_2(20)$ measurements calculated from pH and DIC during EqPac

During OACES EqPac spring and fall-92 spectrophotometric pH measurements were made by the group of Dr. Byrne of the University of South Florida (USF) along 140 °W. These pH values along with the DIC values were used to calculate the $fCO_2(20)$. *Lee and*

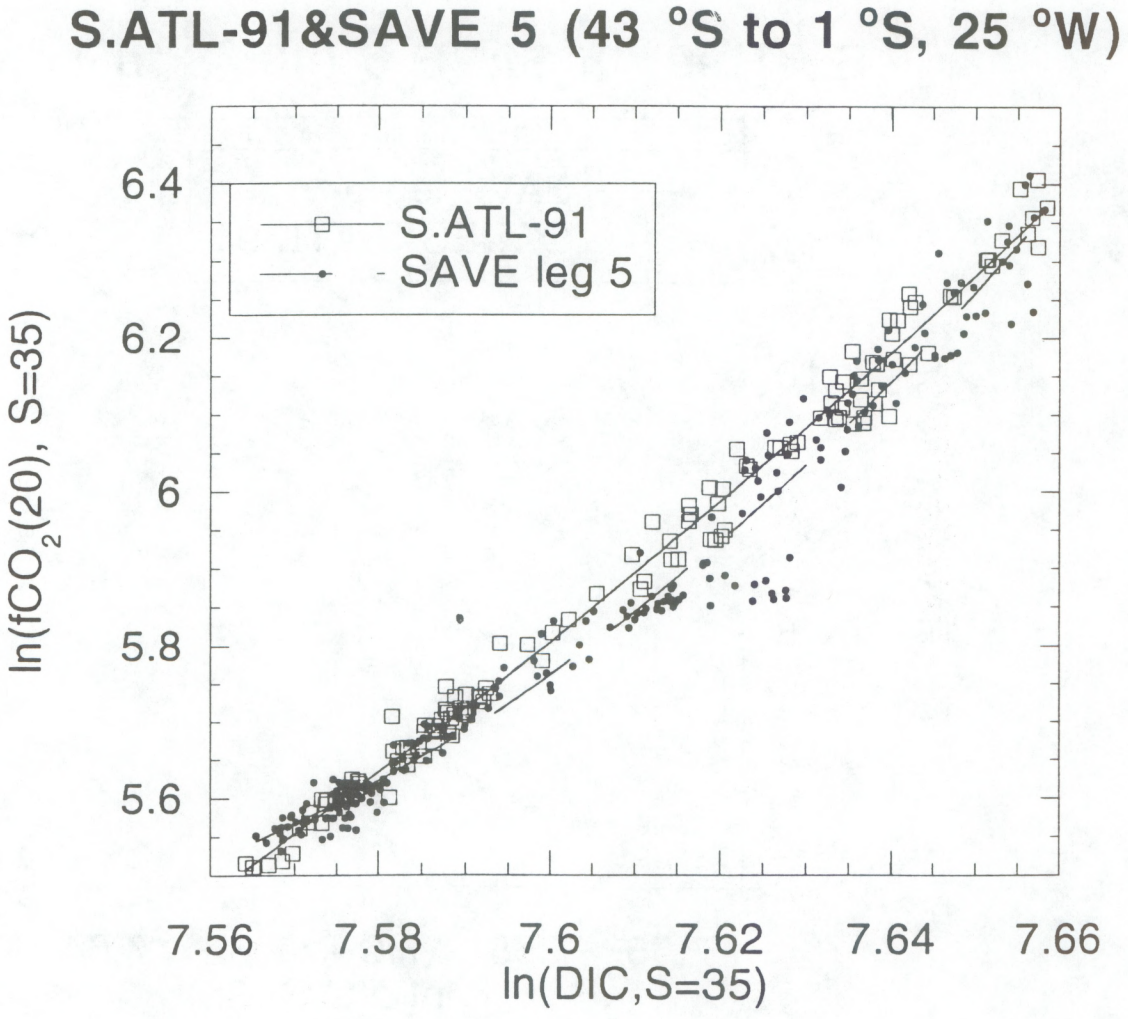

Figure 24. Ln (fCO_2(20),35) vs. ln (DIC,35) for the SAVE and S.ATL-91 cruises. The lines are second-order polynomial least-squares fits through the data points.

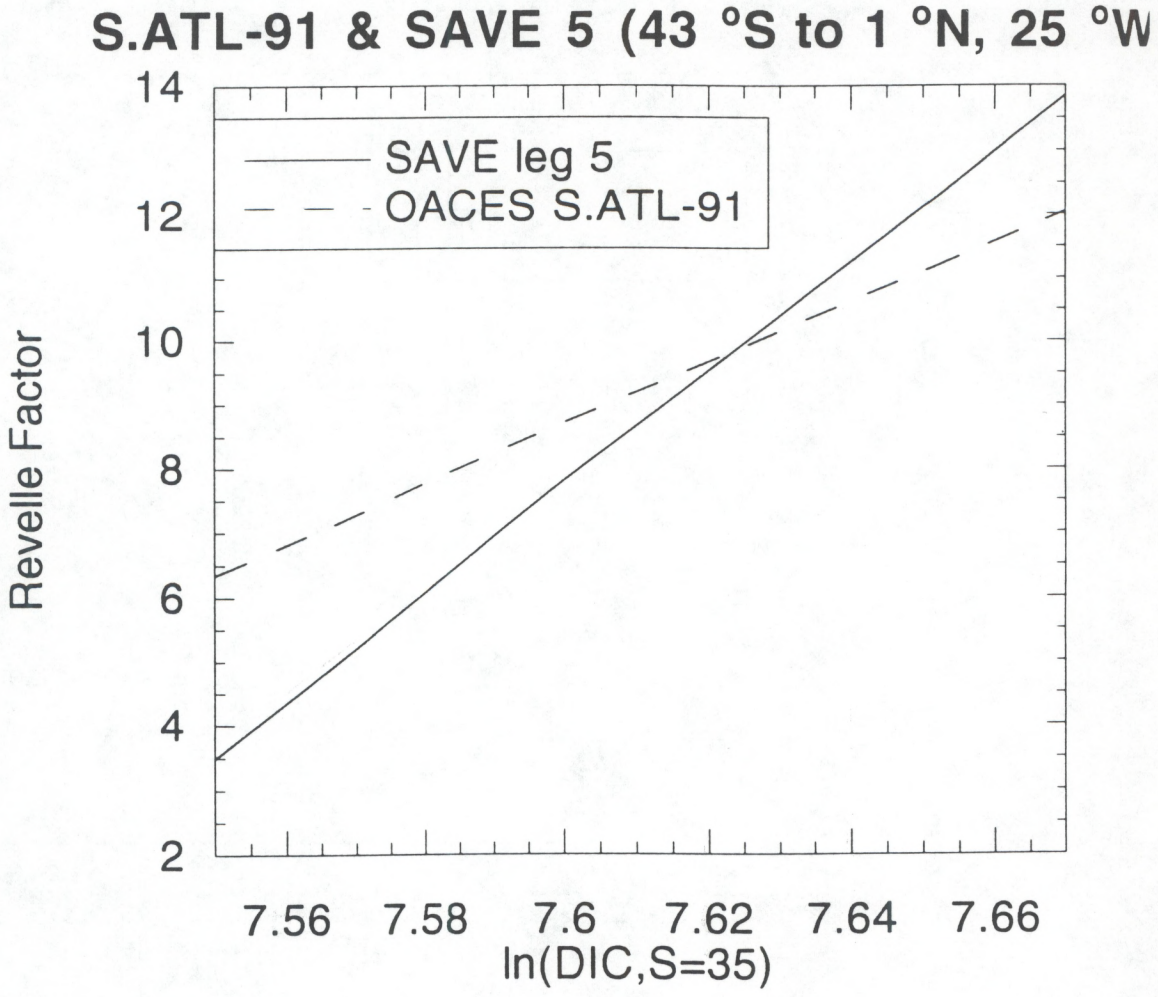

Figure 25. Revelle factor as a function of ln(DIC,35) for SAVE (leg 5)/HYDROS(leg 4) and S.ATL-91 cruises by differentiating the second-order polynomial least squares fits through the data points in Figure 24.

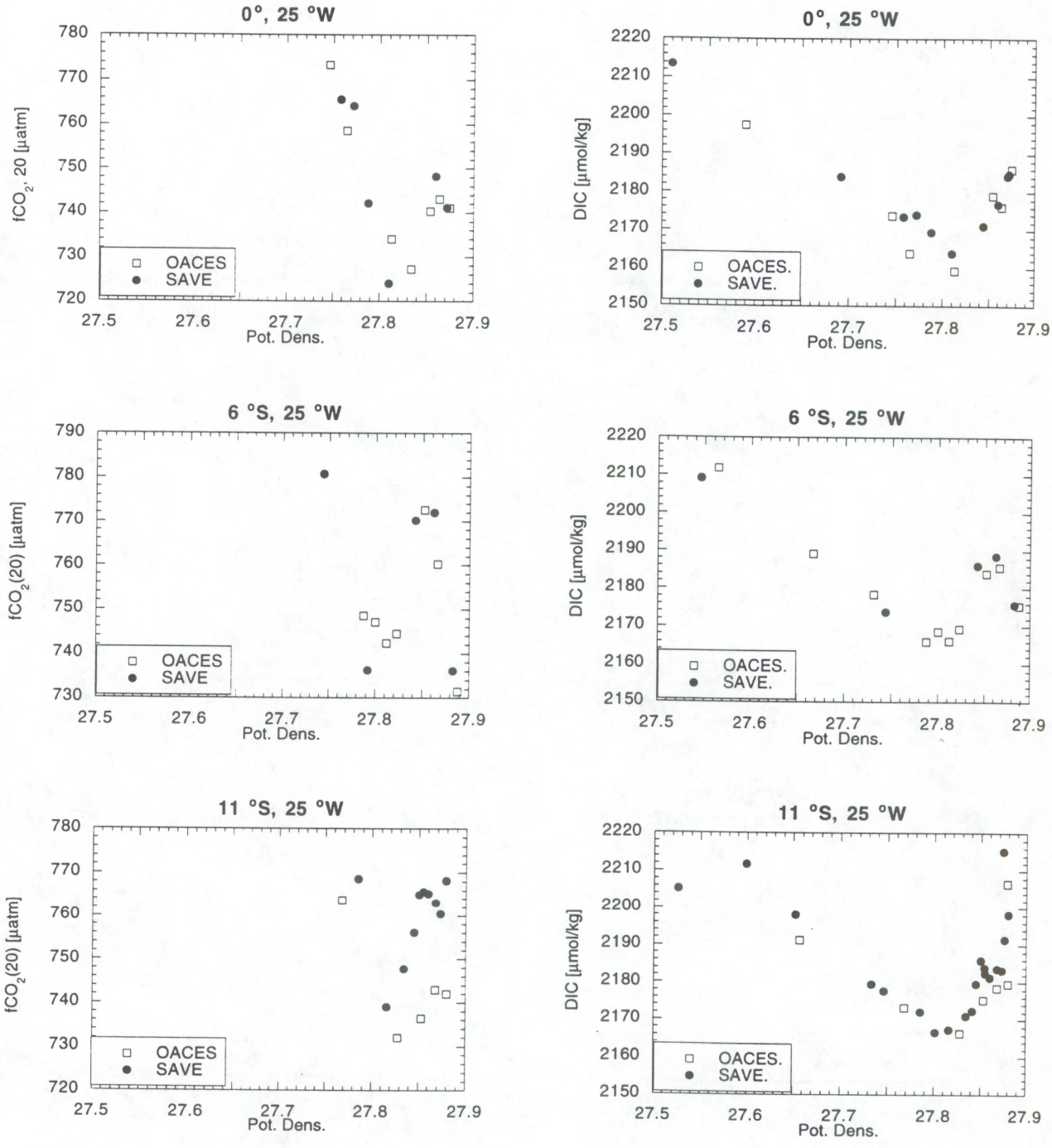

Figure 26. $fCO_2(20)$ and DIC versus potential density in deep water for locations between 0 °N an 11 °S for the SAVE (leg 5)/HYDROS(leg 4) and the S.ATL-91 cruise.

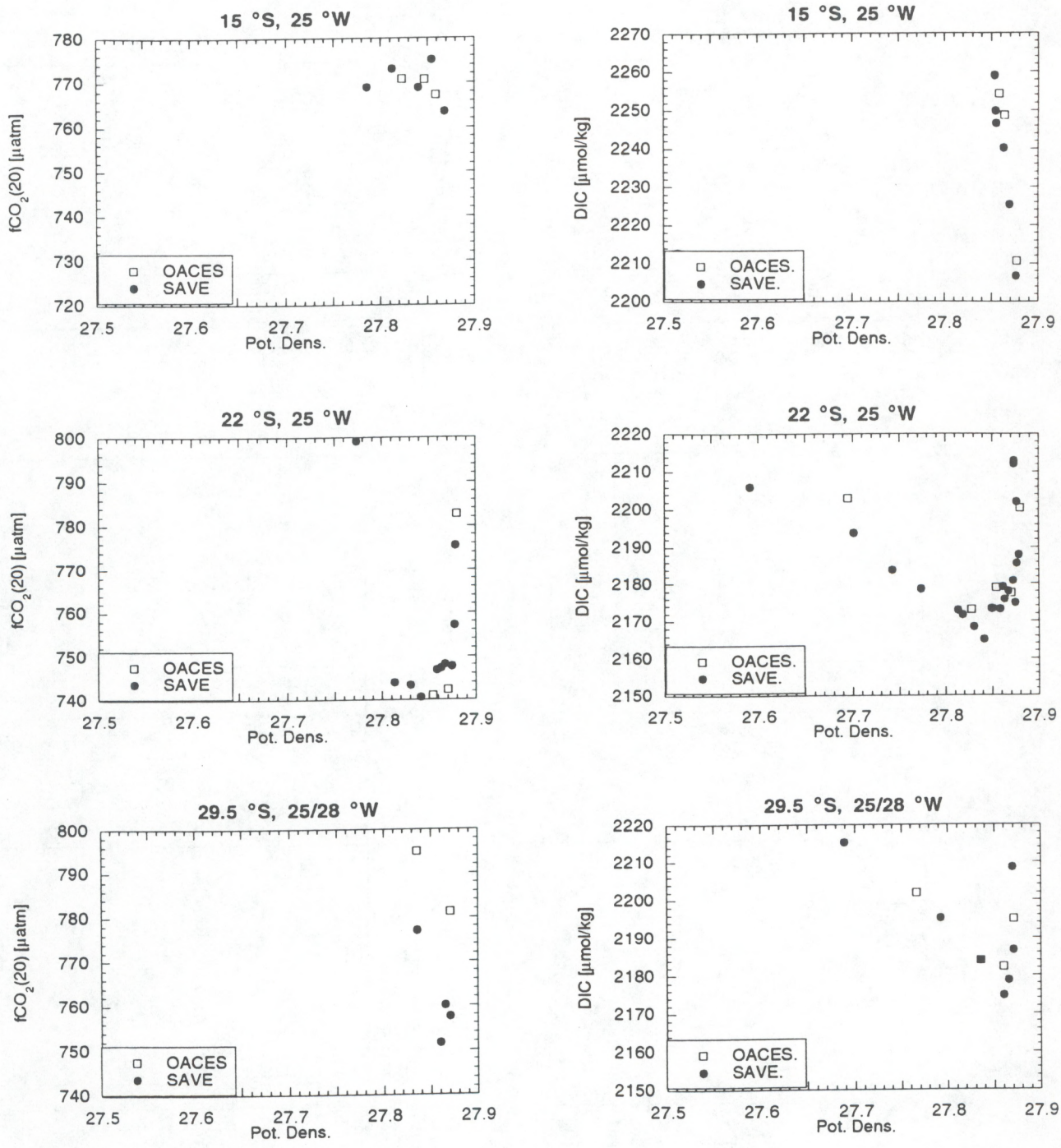

Figure 27. $fCO_2(20)$ and DIC versus potential density locations between 11 °S an 30 °S for the SAVE (leg 5)/HYDROS(leg 4) and the S.ATL-91 cruise.

Millero, in preparation; *Millero*, 1994; and *Millero, et al.*, 1993 have shown that the combination of pH and DIC is particularly sensitive to calculate $fCO_2(20)$. The pH values of Byrne were analyzed at 25 °C and reported on the total pH scale [with H^+ expressed in mol kg^{-1} solution]. The combination of pH and DIC was used to calculate $fCO_2(20)$ using a program supplied by Dr. Millero of RSMAS. The program includes the influence of silicate and phosphate on TAlk values (which was not incorporated in previous versions). Calculations were performed by Mr. Kitack Lee of RSMAS.

For the spring data offsets between measured $fCO_2(20)$ and calculated $fCO_2(20)$ are apparent for each combination of constants described in Table 2. Figure 28 shows the difference between measured and calculated $fCO_2(20)$ using pH and DIC as input parameters for different combinations of constants for depths down to 1000 m. The influence of the different constants (where borate, silicate, and phosphate constants are those presented in Table 2 as " in our work") is apparent. The largest average difference, expressed as ([measured-calculated]/measured value) of about 3.5 to 4 % is observed between measured and the calculated values using the constants of *Dickson and Millero*, [1987]. There is no strong trend of the difference with increasing $fCO_2(20)$ values. The constants of Roy [1993] also yield calculated values greater than those measured with a difference of about 1 % at the surface and 4 % at $fCO_2(20)$ values of 2000 µatm. The calculated values using the carbonate dissociation constants of *Mehrbach et al.*, [1973] yield the smallest difference with on average a 0.5 % offset at 300 µatm and 1.5 % offset at 2000 µatm.

Figure 8 shows the percentage difference plotted against measured $fCO_2(20)$ for the fall. The trends are similar to the results in the spring suggesting that there are no internal biases in the DIC, pH, fCO_2 data between EqPac spring and fall-92. The constants of *Roy* [1993] and *Mehrbach* [1973] again appear to show a depth dependence with better agreement at low $fCO_2(20)$.

Figure 29 shows the pH and measured $fCO_2(20)$ plotted against DIC for thermocline waters. The correlations and standard deviations between pH and DIC, and $fCO_2(20)$ and DIC are very similar. The data also is consistent between spring and fall.

Figure 30 gives the comparison for calculated $fCO_2(20)$ from pH and DIC, and the measured $fCO_2(20)$ for different constants for surface water. The trends are similar for the spring and fall data. The constants of *Mehrbach* [1973] yield the best agreement.

Conclusion

The discrete fCO_2 system using infrared analysis for detection has proven to be a robust instrument for seagoing analyses. Its main drawbacks compared to the systems utilizing a GC, are the relatively large headspace to volume of sample water ratio which causes a large perturbation of fCO_2 during equilibration of deep water, and the decrease in sensitivity at high CO_2 levels due to the non-linearity of the IR detector. However, results indicate that precision is comparable to the GC based systems and cost of hardware and operation is lower. The system has proven to be trouble free and is simple to operate. No conclusive evidence of bias is apparent despite different methods of comparison. The comparisons yield conflicting results, in part because of uncertainty in carbonate dissociation constants. A preliminary side-by-side comparison between discrete GC and IR analyzer based systems based on different operating principles shows no apparent bias. With an increase interest in discrete $fCO_2(20)$ for interpretation of changes in the

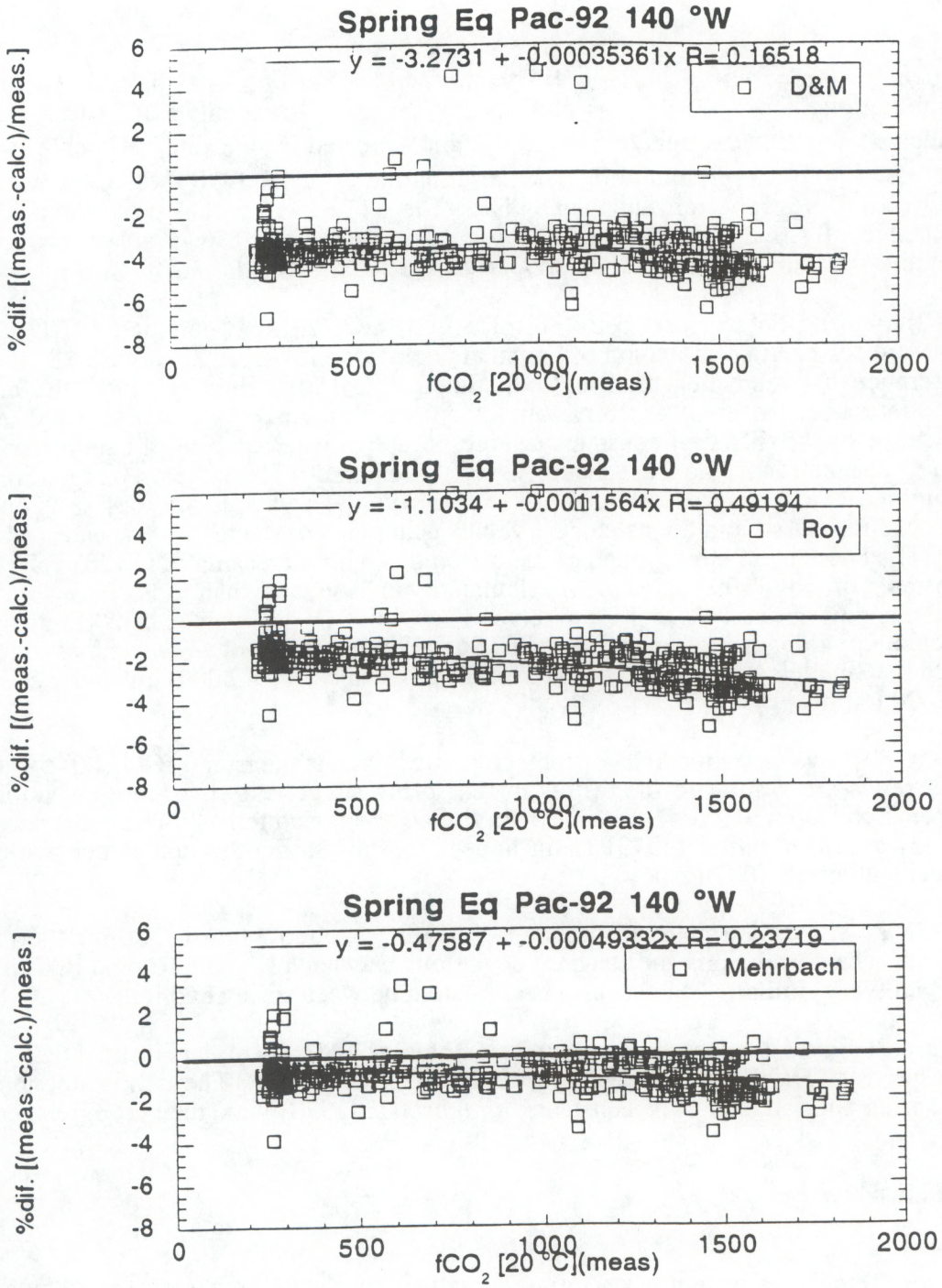

Figure 28. Difference between measured and calculated fCO_2, using pH and DIC as input parameters, for different combinations of constants for EqPac spring-92, 140 °W. D&M=carbon dissociation constants of *Dickson and Millero* [1987]; Mehrbach= constants of *Mehrbach* [1973], and Roy= those of *Roy* [1993].

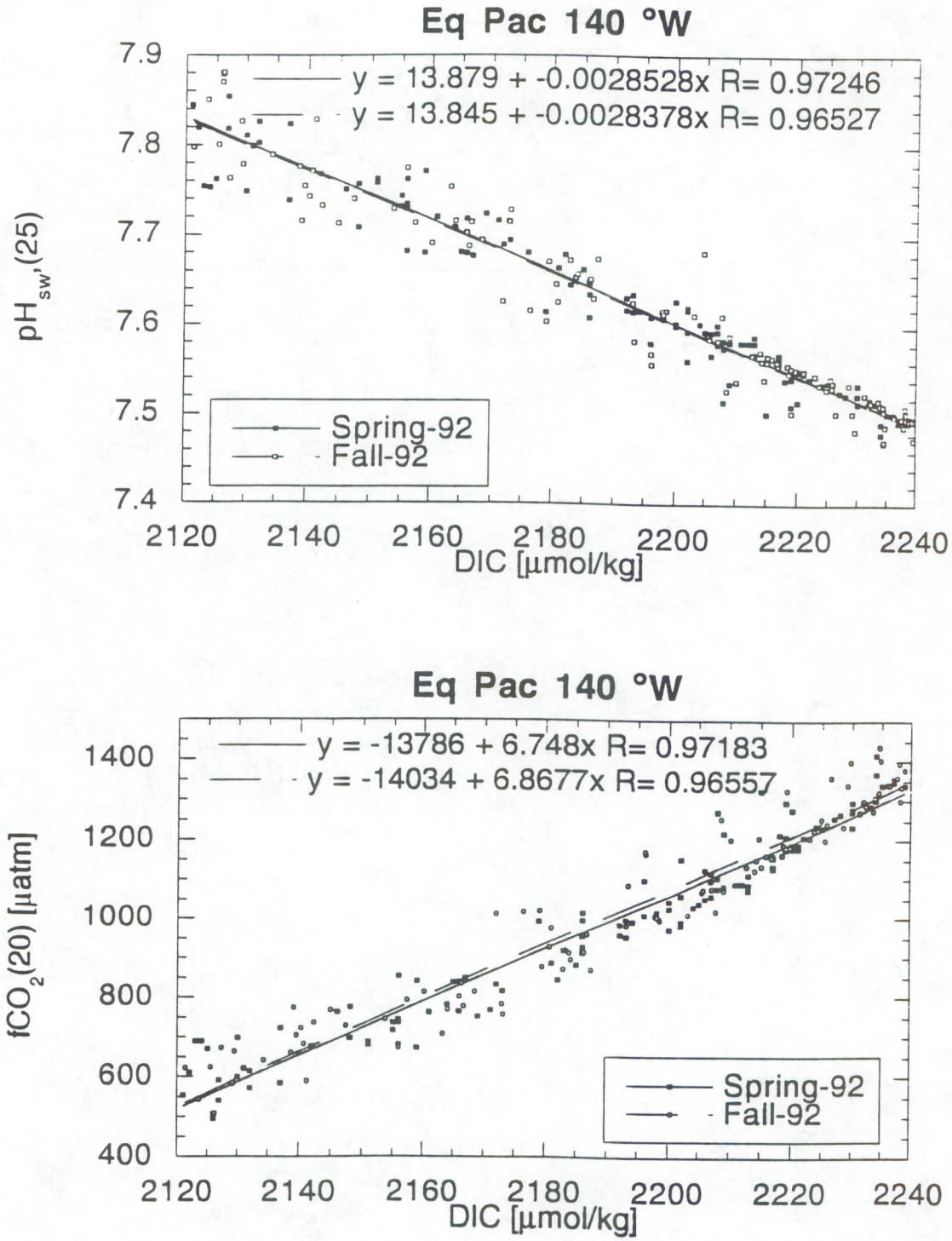

Figure 29. Top: pH plotted against DIC for intermediate waters with DIC content between 2120 and 2240 µmol kg^{-1} for EqPac spring and fall-92. Bottom: $fCO_2(20)$ plotted against DIC for intermediate waters with DIC content between 2120 and 2240 µmol kg^{-1}.

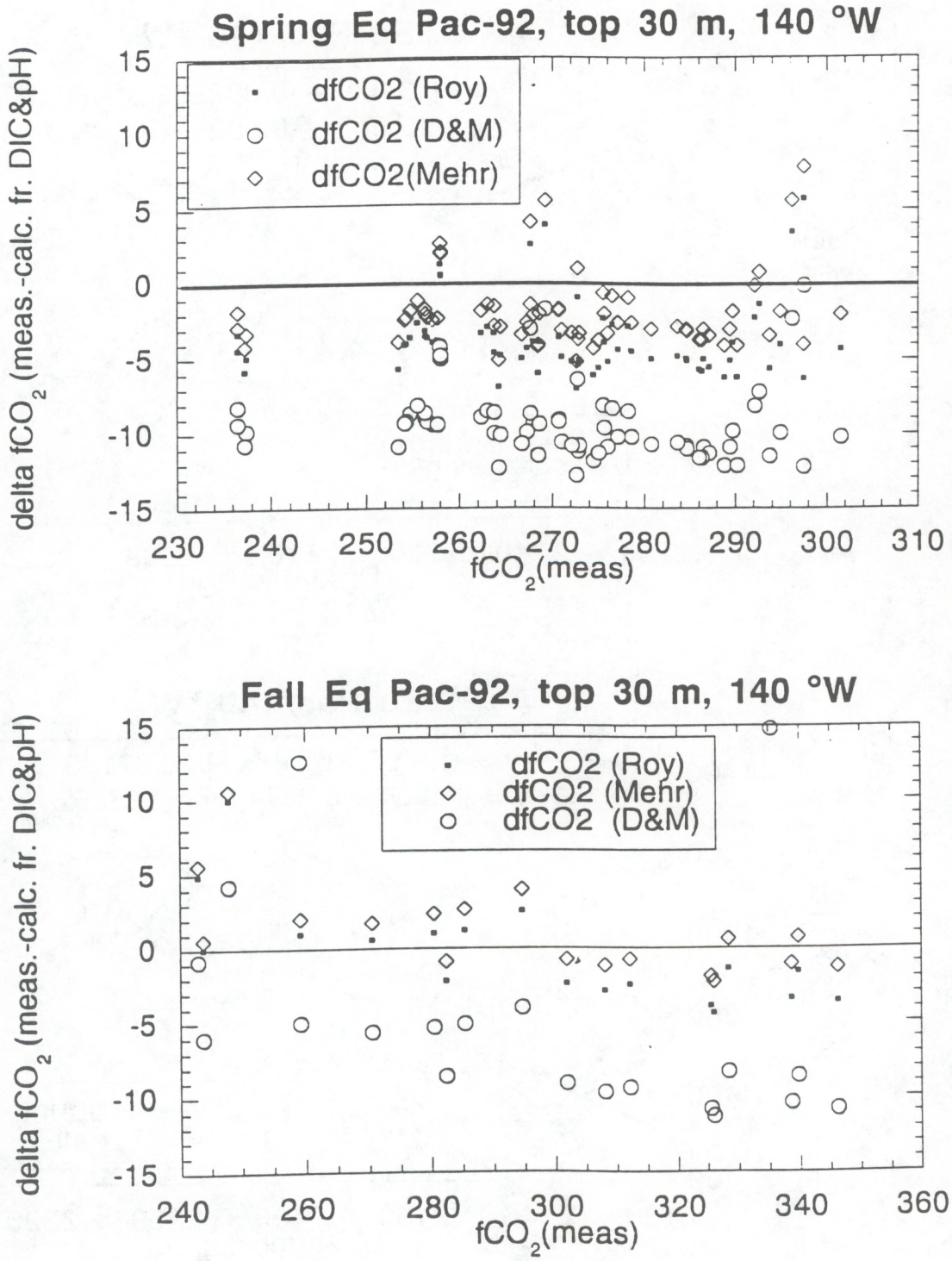

Figure 30. Difference of measured $fCO_2(20)$ and calculated $fCO_2(20)$ from DIC and pH, for samples in the surface mixed layer (0-30 m) for EqPac spring and fall-92.

oceanic carbon reservoir, intercomparisons between different groups would be very timely. This would avoid unreconcilable differences in future work which will complicate creation of uniform global datasets.

Acknowledgment

This work would not have been possible without support of NOAA's Climate and Global Change Program. We wish to thank OACES program manager Dr. James F. Todd, in particular, for funding the fCO_2 work during OACES EqPac-92 and on the OACES long lines. Kitack Lee is gratefully acknowledged for calculating $fCO_2(20)$ from DIC and pH. DIC measurements were performed by Mr. Tom Lantry of AOML, and Ms. Marilyn Roberts of PMEL. Ms. Tonya Clayton and Becky Li, and Drs. Robert Byrne and Jabe Breland of USF performed the pH measurements. Ms. Cathy Cosca of PMEL, and Mr. Matt Steckley, Ms. Molly Knox and Dr. Cathy Ellins were in charge of underway fCO_2 measurements on the different OACES cruises. Their diligence was instrumental in creating a high quality dataset. Drs. Taro Takahashi, and Dave Archer provided the LDEO data which was used in the comparison. H.C. was supported in part by the University of Miami's Cooperative Institute for Marine and Atmospheric Studies under NOAA's cooperative agreement NA37RJ0200

References

Archer, D.E., T. Takahashi, S. Sutherland, J. Goddard, D. Chipman, K. Rodgers, and H. Ogura, Observations of CO_2 Chemistry during the JGOFS Equatorial Pacific Expeditions, 1992: Effect of ENSO on the carbon and nutrient system, *Deep Sea Res., accepted*, 1995.

Byrne, R.H., and J.A. Breland, High precision multiwavelenth pH determinations in seawater using cresol red, *Deep-Sea Research, 36*, 803-810, 1989.

Chipman, D.W., J. Marra, and T. Takahashi, Primary production at 47°N and 20°W in the North Atlantic Ocean: A comparison between the 14C incubation method and mixed layer carbon budget observations, *Deep-Sea Research II, 40*, 151-169, 1993.

Conway, T.J., P.P. Tans, L.S. Waterman, K.W. Thoning, D.R. Kitzis, K.A. Masarie, and N. Zhang, Evidence for interannual variability of the carbon cycle from the NOAA/CMDL global air sampling network, *J. Geophys. Res., 99*, 22831-22855, 1994.

Dickson, A.G., An exact definition of total alkalinity and a procedure for the estimation of alkalinity and total inorganic carbon from titration data, *Deep-Sea Research, 28A*, 609-623, 1981.

Dickson, A.G., Thermodynamics of the dissociation of boric acid in synthetic seawater from 273.15 to 318.15 K, *Deep-Sea Res., 37*, 755-766, 1990.

Dickson, A.G., and F.J. Millero, A comparison of the equilibrium constants for the dissociation of carbonic acid in seawater media, *Deep-Sea Res., 34*, 1733-1743, 1987.

DOE, *Handbook of methods for the analysis of the various parameters of the carbon dioxide system in sea water; version 2*, Dickson, A.G. and C. Goyet, editors, DOE, 1994.

Goyet, C., and A. Poisson, New determination of carbonic acid dissociation constants in seawater as a function of temperature and salinity, *Deep-Sea Res, 36*, 1635-1654, 1989.

Kester, D.R., and R.M. Pytkowicz, Determination of the apparent dissociation constants of phosphoric acid in seawater, *Limnol. Oceanogr., 12*, 243-252, 1967.

LI-COR, LI-6262 CO2/H2O Analyzer Operating and Service Manual, LI-COR, Lincoln, NB, 1990.

Lee, K., and F.J. Millero, Thermodynamics of the carbonate system in the ocean, *Deep-Sea Res.*, in preparation.

Lyman, J., Buffer mechanism of sea water, Univ. of Calif. Los Angeles, 1956.

Mehrbach, C., C.H. Culberson, J.E. Hawley, and R.M. Pytkowicz, Measurement of the apparent dissociation constants of carbonic acid in seawater at atmospheric pressure, *Limnology and Oceanography, 18*, 897-907, 1973.

Millero, F.J., R.H. Byrne, R. Wanninkhof, R. Feely, T. Clayton, P. Murphy, and M.F. Lamb, The internal consistency of CO_2 measurements in the Equatorial Pacific, *Marine Chemistry, 44*, 269-280, 1993.

Millero, F.J., J.-Z. Zhang, K. Lee, and D. Campbell, Titration alkalinity of seawater, *Mar. Chem., 44*, 153-167, 1993.

Neill, C., D.W.R. Wallace, and K.M. Johnson, Small volume, batch equilibration measurement of pCO2 in discrete water samples., *Deep-Sea Res., In preparation*, 1995.

Peng, T.-H., T. Takahashi, W.S. Broecker, and J. Olafsson, Seasonal variability of carbon dioxide, nutrients and oxygen in the northern North Atlantic surface water: observations and a model, *Tellus, 39B*, 439-458, 1987.

Quay, P.D., B. Tilbrook, and C.S. Wong, Oceanic uptake of fossil fuel CO2: Carbon-13 evidence, *Science*, *256*, 74-79, 1992.

Sarmiento, J.L., Oceanic uptake of anthropogenic CO_2: the major uncertainties, *Global. Biogeochemical Cycles*, *5*, 309-313, 1991.

Takahashi, T., P. Kaiteris, W.S. Broecker, and A.E. Bainbridge, An evaluation of the apparent dissociation constants of carbonic acid in seawater, *Earth and Planetary Science Letters*, *32*, 458-467, 1976.

Takahashi, T., J. Olafsson, J.G. Goddard, D.W. Chipman, and S.C. Sutherland, Seasonal variation of CO_2 and nutrients in the high-latitude surface oceans: a comparative study, *Global Biogeochem. Cycles*, *7*, 843-878, 1993.

Tans, P.P., I.Y. Fung, and T. Takahashi, Observational constraints on the global atmospheric CO_2 budget, *Science*, *247*, 1431-1438, 1990.

Wanninkhof, R., and K. Thoning, Measurement of fugacity of CO_2 in surface water using continuous and discrete sampling methods, *Mar. Chem.*, *44* (2-4), 189-205, 1993.

Weiss, R.F., Carbon dioxide in water and seawater: the solubility of a non-ideal gas, *Mar. Chem.*, *2*, 203-215, 1974.

Weiss, R.F., R.A. Jahnke, and C.D. Keeling, Seasonal effects of temperature and salinity on the partial pressure of CO_2 in seawater, *Nature*, *300*, 511-513, 1982.

Weiss, R.F., and B.A. Price, Nitrous oxide solubility in water and seawater, *Mar. Chem.*, *8*, 347-359, 1980.

*U.S. GOVERNMENT PRINTING OFFICE:1995-673-018/00127